Thermal and Urea-Induced Unfolding of the Marginally Stable Lac Repressor DNA-Binding Domain: A Model System for Analysis of Solute Effects on Protein Processes†

Daniel J. Felitsky[#] and M. Thomas Record, Jr.*[,#,‡]

Department of Biochemistry and Department of Chemistry, University of Wisconsin-Madison, Madison, Wisconsin 53706

Received November 1, 2002; Revised Manuscript Received December 17, 2002

ABSTRACT: Thermodynamic and structural evidence indicates that the DNA binding domains of *lac* repressor (lacI) exhibit significant conformational adaptability in operator binding, and that the marginally stable helix−turn−helix (HTH) recognition element is greatly stabilized by operator binding. Here we use circular dichroism at 222 nm to quantify the thermodynamics of the urea- and thermally induced unfolding of the marginally stable lacI HTH. Van't Hoff analysis of the two-state unfolding data, highly accurate because of the large transition breadth and experimental access to the temperature of maximum stability (T_S; 6−10 °C), yields standard-state thermodynamic functions (ΔG°_{obs}, ΔH°_{obs}, ΔS°_{obs}, $\Delta C^\circ_{P,obs}$) over the temperature range 4−40 °C and urea concentration range $0 \leq C_3 \leq 6$ M. For unfolding the HTH, ΔG°_{obs} decreases linearly with increasing C_3 at all temperatures examined, which directly confirms the validity of the linear extrapolation method (LEM) to obtain the intrinsic stability of this protein. At 25 °C (pH 7.3 and 50 mM K^+), both linear extrapolation and extrapolation via the local-bulk domain model (LBDM) to $C_3 = 0$ yield $\Delta G^\circ_{obs} = 1.23 \pm 0.05$ kcal mol^{-1}, in agreement with direct measurement (1.24 ± 0.30 kcal mol^{-1}). Like ΔG°_{obs}, both ΔH°_{obs} and ΔS°_{obs} decrease linearly with increasing C_3; the derivatives with respect to C_3 of ΔG°_{obs}, ΔH°_{obs} and $T\Delta S^\circ_{obs}$ (in cal mol^{-1} M^{-1}) are -449 ± 11, -661 ± 90, and -203 ± 91 at 25 °C, indicating that the effect of urea on ΔG°_{obs} is primarily enthalpic. The $\Delta C^\circ_{P,obs}$ of unfolding (0.63 ± 0.05 kcal mol^{-1} K^{-1}) is not detectibly dependent on C_3 or temperature. The urea *m*-value of the lacI HTH ($-d\Delta G^\circ_{obs}/dC_3 = 449 \pm 11$ cal mol^{-1} M^{-1} at 25 °C) is independent of C_3 up to at least 6 M. Use of the LBDM to fit the C_3-dependence of ΔG°_{obs} yields the local-bulk partition coefficient for accumulation of urea at the protein surface exposed upon denaturation: $K_P = 1.103 \pm 0.002$ at 25 °C. This partition coefficient is the same within uncertainty as those previously determined by LBDM analysis of osmometric data for solutions of urea and native (folded) bovine serum albumin, as well as LBDM analysis of the proportionality of *m*-values to changes in water accessible surface area upon protein unfolding. From the correspondence between values of K_P, we conclude that the average local urea concentration at both folded and unfolded protein surface exceeds the bulk by approximately 10% at 25 °C. The observed decrease in *m*-value for the lacI HTH with increasing temperature, together with the observed reductions in both ΔH°_{obs} and ΔS°_{obs} of unfolding with increasing urea concentration, demonstrate that K_P for urea decreases with increasing temperature and that transfer of urea from the bulk solution to the local domain at the protein surface exposed on denaturation is enthalpically driven and entropically unfavorable.

The *lac* repressor (lacI)−operator DNA interaction, a prototype system for regulation of gene expression and one of the most specific protein−DNA interactions, has also been a model for biophysical studies of the roles of major coupled conformational changes in both the protein and the DNA in site-specific binding. In addition to the observed ∼40° bend observed in the symmetric (SymL) operator DNA (*1*), proposed large scale conformational changes linked to operator binding include wrapping (*2*, *3*) and looping (*4*, *5*) of flanking DNA regions and folding (*6*, *7*) and conformational adaptability (*8*−*10*) of elements of the lacI DNA-binding interface, formed by the DNA binding domains (DBD)[1] of two subunits of the lacI tetramer. Each DBD consists of a 49-residue helix−turn−helix (HTH) domain connected to the core protein by a ∼13-residue hinge region which is helical in a complex of the DBD with a tight-binding operator (*11*, *12*) but unfolded in the free DBD (*7*) and in a complex with weak-binding operator variant (*12*, *13*). Comparative thermodynamic studies of interactions of the lacI tetramer with wild type and variant operators (*8*, *10*) led to the proposals that extensive folding of elements of

† This research was supported by NIH Grants GM47022 and GM23467.

* Corresponding author: 433 Babcock Dr., Madison, WI 53706. E-mail: record@biochem.wisc.edu.

[#] Department of Biochemistry.

[‡] Department of Chemistry.

[1] Abbreviations: lacI DBD, lac repressor DNA-binding domain; HTH, helix−turn−helix domain; CD, circular dichroism.

10.1021/bi0270992 CCC: $25.00
Published on Web 02/01/2003

the DBD is coupled to specific binding (*6*) and that conformational adaptability, including sequence-specific differences in the extent of folding, results in different protein conformations in complexes with different operator sequences (*8*, *10*). Recently, a direct demonstration of operator sequence-specific differences in the extent of folding of the hinge helices in binding to symmetric and natural operators has been obtained from elegant NMR structural characterization of complexes formed by a cross-linked dimer of the DBD. Protection factors for exchangeable protons in the HTH increase from $\sim 10^2$ to as large as $\sim 10^8$ upon binding to SymL (*14*); protection factors of exchangeable protons in the region of the hinge helix are undetectably small in the unbound state and increase to $\sim 10^5$ upon SymL binding. The hinge region is unfolded in the unbound state of the DBD under all conditions investigated, including low temperature and high salt concentration, as confirmed in the present work. The marginal stability of the HTH and the instability of the hinge helices have been proposed to play important roles in operator recognition (*15*). Early thermodynamic studies of stability of the HTH (obtained by limited proteolysis of intact tetrameric repressor) provided only fragmentary and in some cases conflicting information. The present study is a comprehensive thermodynamic investigation of thermal unfolding of the lacI HTH over a wide range of urea concentrations, quantifying both the marginal stability of this protein domain and the thermodynamic basis of the action of urea as an unfolding solute.

The perturbing solute urea has been widely used in studies of intrinsic thermodynamic stability (ΔG°_{obs}) (*16*, *17*) and intrinsic rate constants (*18*) of folding and unfolding of proteins and of the differences in stability and cooperativity for site-specific protein mutants (*19*, *20*), as well as in characterizations of the denatured state (*16*, *19*, *21*). Thermodynamic and kinetic analyses require extrapolation of free energy data from the transition region, which is generally above 4 M urea, to zero urea concentration. The most widely used method of extrapolation is the empirical linear extrapolation method (LEM), first proposed by Greene and Pace (*22*), which assumes a linear dependence of ΔG°_{obs} on the molar concentration of denaturant. For most proteins, the assumption of linearity cannot be tested directly in the temperature and pH range of interest. Attempts to investigate the linearity of the extrapolation of ΔG°_{obs} to zero urea concentration using a second perturbing variable (e.g., temperature, pH) have reached different conclusions with different proteins (linear (e.g., *23*, *24*), nonlinear (e.g., *25*, *26*)).

In general, an *m*-value for urea (or the corresponding free energy derivative for any other nonelectrolyte solute) is most fundamentally and rigorously interpreted in terms of the corresponding model-independent difference in thermodynamic preferential interaction coefficients ($\Delta\Gamma$) characterizing the interactions of urea with unfolded and folded states (*27*−*30*). This difference is equivalent (assuming additivity of interactions) to the preferential interaction coefficient of urea with the subset of protein surface which is exposed on unfolding (*31*). Thermodynamic data for interactions of urea with protein surface and model compounds have been interpreted using various site-binding models (*32*, *33*) and, most recently, by a local-bulk partitioning model in which the distribution of urea between the surface of the protein (local domain) and the bulk solution is described by a urea concentration-independent partition coefficient K_P (*31*).

To characterize the thermodynamic basis of the marginal stability of the lacI HTH and to perform direct experimental tests of the LEM and of the application of local-bulk domain model (LBDM) for urea effects, we have quantified the thermal unfolding transition of this marginally stable HTH domain as a function of urea concentration using circular dichroism. Thermal unfolding of the lacI HTH is well described thermodynamically as a cooperative two-state process, which allows an unambiguous determination of its thermodynamics of denaturation. As observed for some other small proteins and α-helical peptides (e.g., *34*), where both the enthalpy of unfolding at the transition temperature (T_G^H) and the increase in water-accessible surface area upon unfolding are small, the lacI HTH exhibits relatively broad thermal and urea-induced unfolding transitions. Because of its marginal stability and broad transitions, K_{obs} and ΔG°_{obs} of unfolding of lacI HTH are directly measurable at neutral pH over a much wider range of urea concentrations and temperatures than are accessible for most proteins, including 25 °C in the absence of urea. Consequently ΔH°_{obs}, ΔS°_{obs}, and $\Delta C^\circ_{P,obs}$ are accurately determined by van't Hoff analysis. Interpretation of the data using the LBDM for the partitioning of urea between the protein surface and the bulk solution yields a quantitative description of the interaction of urea with the surface exposed upon unfolding.

Background on Preferential Interaction Coefficients and the Local-Bulk Domain Analysis of m-Values. The general thermodynamic result for the dependence of the observed equilibrium constant K_{obs} for two-state unfolding of a protein on the activity (a_3) of a nonelectrolyte solute such as urea (present in excess in a three-component system) is the following:

$$\left(\frac{\partial \ln K_{obs}}{\partial \ln a_3}\right)_{T,P} = \Delta\Gamma_{\mu_3} \qquad (1)$$

where $\Delta\Gamma_{\mu_3}$ is the stoichiometrically weighted difference in preferential interaction coefficients Γ_{μ_3} characterizing interactions of urea with the unfolded and the folded protein ($\Gamma_{\mu_3} \equiv (\partial m_3/\partial m_2)_{T,P,\mu_3}$) (*27*−*30*). Molal concentrations of the protein and of any buffer or salts (if present) are maintained constant in the derivative in eq 1. Where urea is in excess, fourth-component effects on this derivative can be neglected, as can any possible effects of protein concentration on Γ_{μ_3} (D.J.F., unpublished).

Protein unfolding studies have historically expressed urea concentration on the molar scale (C_3), on which scale urea in water behaves relatively ideally ($\gamma^c_{urea} \sim 1$) even at molar concentrations (*35*), and have defined the *m*-value as the negative of the slope of a plot of the standard free energy change ΔG°_{obs} of unfolding vs C_3 (*36*):

$$m\text{-value} \equiv -\left(\frac{\partial \Delta G^\circ_{obs}}{\partial C_3}\right)_{T,P} = RT\left(\frac{\partial \ln K_{obs}}{\partial C_3}\right)_{T,P} \qquad (2)$$

In these studies, the concentration of urea (C_3) greatly exceeds the concentrations of protein and of any buffer and salt components, which are held constant. Within uncertainty, the *m*-value for protein unfolding is independent of C_3 in the observable concentration range (which, for typical

proteins, covers a 2 M window in the range 4−9 M urea). From eqs 1 and 2, a model-independent thermodynamic relationship between the experimental *m*-value and the difference in urea−protein preferential interaction coefficients for unfolded and folded states ($\Delta\Gamma_{\mu_3}$) is obtained (*31*). Except for a relatively small nonideality correction, the *m*-value is proportional to the quotient $\Delta\Gamma_{\mu_3}/C_3$.

For all weakly interacting solutes, including both protein stabilizers (e.g., glycine betaine and other osmolytes) and destabilizers (e.g., urea, guanidinium salts), the LBDM provides a quantitative interpretation of Γ_{μ_3} (characterizing a solute-biopolymer interaction) and $\Delta\Gamma_{\mu_3}$ (characterizing the effect of solute concentration on a biopolymer process; cf. eq 1) in terms of the partitioning of the solute between the local domain adjacent to the biopolymer surface and the bulk solution domain where solute and solvent are unperturbed by the presence of biopolymer (*31*, *37*, *38*). The local-bulk partition coefficient of the solute, K_P, is defined as the ratio of the molalities of solute component 3 in the local and bulk domains:

$$K_P \equiv \frac{m_3^{local}}{m_3^{bulk}} \tag{3}$$

Courtenay et al. (*31*, *39*) recently determined partition coefficients for the interaction of urea with folded (F) and unfolded (U′) protein surface. Analysis of vapor pressure osmometry measurements on urea−BSA solutions (0−1 M urea) yielded $K_{P,urea}^{F} = 1.10 \pm 0.04$, independent of urea concentration in this range. Analysis of the proportionality of urea *m*-values to the ΔASA of unfolding reported by Myers et al. (1995) yielded $K_{P,urea}^{U'} = 1.12 \pm 0.01$ at higher urea concentration. Courtenay et al. (*31*) therefore concluded that urea denaturation reflected only the difference in quantity and not a difference in quality of interactions of urea with the unfolded state and explained the identical K_P values for folded and unfolded protein surface by the observation that the contribution of polar peptide backbone to the water accessible surface is the same (∼13%) for both folded and unfolded states. This value of K_P (1.12 ± 0.01) indicates that, on average, the local concentration of urea at the surface of a typical folded or unfolded protein is 11−13% higher than its bulk concentration. For the microscopic process of transferring urea into the local domain from bulk solution, we define a standard free energy change $\Delta G_P^\circ \equiv -RT \ln K_P$. The temperature dependences of K_P and ΔG_P° then yield the enthalpic and entropic contributions to the solute transfer process.

In the local-bulk thermodynamic analysis, the preferential interaction coefficient Γ_{μ_3} is most directly related to K_P by the molal-scale expression (*31*):

$$\frac{\Gamma_{\mu_3}}{m_3^{bulk}} = \frac{(K_P - 1) b_1^\circ \, ASA}{m_1^\bullet (1 + K_P S_{1,3} m_3^{bulk} m_1^{\bullet -1})} \tag{4}$$

where b_1° is the amount of water in the local domain per unit of biopolymer surface in the absence of solute (expressed as water molecules per Å^2), $m_1^\bullet = 55.5$ mol/kg is the molal concentration of water, and $S_{1,3}$ is the cumulative exchange stoichiometry (the ratio of the number of water molecules displaced to the number of solute molecules present in the local domain). Where the concentration of urea is in vast excess over that of the biopolymer, as is invariably the case in protein folding studies, m_3^{bulk} is accurately approximated by m_3. The combination of eqs 1−4 yields the local-bulk domain interpretation of the urea *m*-value:

$$\frac{m\text{-value}}{RT} = \frac{(K_P - 1) b_1^\circ \, ASA^{U'}}{m_1^\bullet (1 + K_P S_{1,3} m_3 m_1^{\bullet -1})} (1 + \epsilon_3^m) \left(\frac{\partial m_3}{\partial C_3}\right)_{T,P} \tag{5}$$

where ϵ_3^m represents the derivative $d\ln \gamma_3^m / d\ln m_3$ (where γ_3^m is the molal scale activity coefficient of urea), $ASA^{U'}$ is the accessible surface area exposed on unfolding, and the quantities K_P, b_1° and $S_{1,3}$ refer to that surface. For unfolding experiments in excess urea at constant protein and buffer concentrations, the concentration scale conversion $(\partial m_3/\partial C_3)_{T,P}$ in eq 5 can be accurately approximated by its value in a two-component urea−water mixture. (The corresponding molar scale expression was given in ref *31*.)

The intrinsic stability ΔG_{obs}° of a typical globular protein at 25 °C is normally determined by linear extrapolation of urea denaturation data (LEM) or by nonlinear extrapolation of thermal denaturation data, typically using a temperature-independent $\Delta C_{P,obs}^\circ$. For a marginally stable protein like the lacI DBD, ΔG_{obs}° is also directly determined at 25 °C. In addition, ΔG_{obs}° can be obtained by integration of urea denaturation data using the LBDM by combining eqs 2 and 5:

$$\Delta G_{obs}^\circ = \Delta G_{obs}^\circ (m_3 = 0) + m_1^{\bullet -1} RT (K_P - 1) b_1^\circ \, ASA^{U'} \int_0^{m_3} \frac{(1 + \epsilon_3^m) dm_3}{(1 + K_P S_{1,3} m_1^{\bullet -1} m_3)} \tag{6}$$

Values of ϵ_3^m as a function of urea molality at temperatures in the range 2−40 °C are obtained from the data of Stokes (*35*; see Methods for Polynomial Fitting).

Temperature derivatives of ΔG_{obs}° yield ΔH_{obs}°, ΔS_{obs}° and $\Delta C_{P,obs}^\circ$ of unfolding. Likewise, the temperature derivatives of the *m*-value and of the related derivative $\partial \ln K_{obs}/\partial C_3$ provide information about the thermodynamic basis of urea partitioning in the vicinity of the protein surface area ($ASA^{U'}$) exposed on unfolding. From the equality of second partial derivatives of a function irrespective of order of differentiation with respect to temperature and urea concentration, applied to ΔG_{obs}°, $\ln K_{obs}$, ΔH_{obs}°, and ΔS_{obs}°:

$$\left(\frac{\partial m\text{-value}}{\partial T}\right)_{C_3} = \left(\frac{\partial \Delta S_{obs}^\circ}{\partial C_3}\right)_T \tag{7}$$

$$\left(\frac{\partial}{\partial T}\left(\frac{\partial \ln K_{obs}}{\partial C_3}\right)_T\right)_{C_3} = \frac{1}{RT^2}\left(\frac{\partial \Delta H_{obs}^\circ}{\partial C_3}\right)_T \tag{8}$$

$$\left(\frac{\partial}{\partial T}\left(\frac{\partial \Delta H_{obs}^\circ}{\partial C_3}\right)_T\right)_{C_3} = \left(\frac{\partial \Delta C_{P,obs}^\circ}{\partial C_3}\right)_T = T\left(\frac{\partial}{\partial T}\left(\frac{\partial \Delta S_{obs}^\circ}{\partial C_3}\right)_T\right)_{C_3} \tag{9}$$

Equations 7−9 would be exact if a molal concentration scale were used for urea; since the partial molar volume of urea

is somewhat temperature dependent (*35*), these molar-scale expressions are approximate, though the correction terms are small in the range of interest (D.J.F., unpublished).

METHODS

Chemicals. Anhydrous K_2HPO_4 (99.7% pure, FW 174.18), certified ACS grade KCl (99.9% pure, FW 74.56), and electrophoresis grade urea (>99% pure, FW 60.06) were obtained from Fisher Scientific (Pittsburgh, PA) and used without further purification. Proteinase K was obtained from Worthington Biochemical (Lakewood, NJ). Distilled deionized water was used in all experiments. Other chemicals were reagent grade.

Purification of the 62 Residue Lac Repressor DNA-Binding Domain. *Escherichia coli* DH9 cells containing the pGP1−2 and pEt-3a-HP62 plasmids were obtained from Drs. C. A. E. M. Spronk and R. L. Kaptein (University of Utrecht). Expression and purification were performed as described for the 56-residue lacI DBD (*40*), except that Sephacryl 100 was used in place of Sephadex 50 and SP sepharose was used as the cation-exchange resin. Elution of the cation exchange column yielded two significant peaks; the second of these, eluting at 0.6 M KCl, is homogeneous 62-mer, as judged from an overloaded 16.5% Tris-Tricine SDS−polyacrylamide gel, which showed a single band of approximately 7 kDa molecular mass. Electrospray mass spectroscopy analysis of the purified 62-mer yielded a molecular weight of 6753.9 in agreement with that calculated from the sequence. A molar extinction coefficient of 5400 M^{-1} at 280 nm (Dr. C. A. E. M. Spronk, personal communication) was used in determining concentrations of the 62-residue lacI DBD.

Preparation of Protein Solutions for CD Studies. LacI DBD was dialyzed at least 24 h at 4 °C in tubing of MWCO 1000 or 3500 with a single change at 12 h of a >1000-fold excess of 25 mM K_2HPO_4, pH 7.3 (adjusted using HCl) and either 0, 8.0, or 9.1 M urea. Extending the dialysis period to 48 h had no significant effect on the CD measurements. At lower concentrations of K_2HPO_4, the protein precipitated upon prolonged dialysis. A stock solution of 2, 4, or 8 M urea and 25 mM K_2HPO_4 was prepared volumetrically immediately before use and adjusted to pH 7.3 using HCl. For experiments below 6 M urea, 100 μL of protein stock was combined with appropriate amounts of urea stock (e.g., 4 M) and K_2HPO_4 dialysis buffer to a total volume of 300 μL in 1.0 mm path length stoppered cuvettes. To prepare solutions at higher urea concentrations, we took advantage of the complete reversibility of unfolding at low temperature and diluted samples of unfolded lacI DBD in 8.0 or 9.1 M urea buffer with K_2HPO_4 dialysis buffer. Control experiments for samples prepared by both methods at urea concentrations in the range 1.6−2.0 M and 4−5 M urea gave the same unfolding curves within uncertainty. The concentration of K^+ was 50 mM in all CD studies of urea induced unfolding reported here. To stabilize the folded state and establish its baseline (cf. Appendix), the salt concentration was increased with KCl.

Circular Dichroism Spectroscopy. Circular dichroism spectroscopy monitored at 222 nm was performed on an Aviv 62A DS CD spectrometer with a multicell attachment allowing simultaneous heating of five cuvettes. Heating curves typically spanned the range 3.6−98.4 °C and used the same series of temperature steps (~3 °C). Thermal equilibration after each step was achieved in less than 8 min. After equilibration, samples were thermostated at the desired temperature (within a ± 0.2 °C instrumental deadband) for one minute before readings were taken. Reducing the 0.2 °C deadband to 0.1 °C required significantly longer equilibration times (~15 min) but did not affect the shape of the heating curves or the transition midpoint. Use of a 0.2 °C deadband introduces an uncertainty of ± 0.2 °C in all temperatures reported herein. Corrections for differences in temperature between the block and the sample cells were made by comparing instrument temperature readings with those made by a thermocouple inserted into one of the cells. This correction was significant (e.g., 3.5 °C at 95 °C), with the largest corrections occurring at the extremes of the temperature range. Data collected from replicate samples placed in different positions in the cell holder agreed within the tolerance expected for replicate samples in the same cell position. Cooling the samples to 4 °C after performing thermal melts to 98 °C leads to greater than 90% recovery of signal (as judged by both ellipticity at 222 nm and wavelength scans of the protein from 200 to 260 nm). Signal recovery is improved to greater than 99% by stopping the thermal melts at 80 °C. Repeat melts of these samples behaved identically to the initial melts with no alteration in the shape or midpoint of the transition curve. Reversibility of urea denaturation at low temperature was assessed by diluting samples dialyzed against concentrated urea (8.0 or 9.1 M) to 1.6−6.0 M urea and comparing the results with samples prepared by addition of urea to samples dialyzed against buffer. Agreement between these methods indicates that urea denaturation is also greater than 99% reversible. Buffer-only controls over the entire range of urea concentrations showed no dependence on temperature. Rather than increase the random noise in the data by subtracting these blanks, a small arbitrary *y*-axis offset was included in the baseline fitting to account for day-to-day variations in the instrument base signal. This offset correction, applied consistently throughout this study, has no effect on our results. Generally, between three and five replicates were averaged for each set of solution conditions (see Table 1).

To aid in establishing a CD baseline for the unfolded state, exhaustive proteinase K digests of the lacI DBD were performed in our standard 25 mM K_2HPO_4 buffer, pH 7.3, and 1.0 mM $CaCl_2$. Reaction progress was followed by monitoring ellipticity at 222 nm at 25 °C until no further change in signal was observed. From the number and distribution of cleavage sites for proteinase K in the lacI HTH sequence, we predict that no peptide fragment exceeds six residues in length.

Calculation of K_{obs} and ΔG°_{obs} from CD Data. Circular dichroism data at 222 nm were converted to mean residue ellipticity ($[\theta]^{obs}_{222}$) (*41*), and the fraction (f_U) of HTH residues in the unfolded state was calculated from eq 10:

$$f_U = \frac{[\theta]^{obs}_{222} - [\theta]^{F}_{222}}{[\theta]^{U}_{222} - [\theta]^{F}_{222}} \quad (10)$$

In eq 10, experimentally determined universal baselines with quadratic and linear temperature dependences for the post-transition and pre-transition regions, respectively (see

Table 1: Thermodynamic Parameters Describing the LacI DBD Unfolding Transition at Various Urea Concentrations

						at 25 °C		
[urea] (M)	# expts	$\Delta C^{\circ}_{P,obs}$ (cal mol^{-1} K^{-1})	T^{H}_{G} (°C)	T_S (°C)	T_H (°C)	ΔG°_{obs} (cal mol^{-1})	ΔH°_{obs} (cal mol^{-1})	ΔS°_{obs} (cal mol^{-1} K^{-1})
0.0	9	627 ± 139	45.6 ± 0.2	7.8 ± 1.5	5.3 ± 1.7	1240 ± 301	12394 ± 1987	37.4 ± 6.7
0.4	3	634 ± 59	43.0 ± 0.1	9.1 ± 0.5	7.1 ± 0.6	998 ± 91	11395 ± 660	34.9 ± 2.2
0.8	5	618 ± 36	40.4 ± 0.1	6.0 ± 0.3	3.9 ± 0.3	893 ± 61	13061 ± 273	40.8 ± 0.9
1.2	5	636 ± 31	37.5 ± 0.1	7.2 ± 0.3	5.6 ± 0.3	672 ± 48	12395 ± 305	39.3 ± 1.0
1.6	5	627 ± 87	35.0 ± 0.1	6.0 ± 0.7	4.6 ± 0.8	527 ± 107	12825 ± 689	41.2 ± 2.3
2.0	2	613 ± 62	31.2 ± 0.1	6.8 ± 0.6	5.7 ± 0.6	286 ± 53	11853 ± 404	38.8 ± 1.4
2.7	3	642 ± 46	24.8 ± 0.1	7.3 ± 0.3	6.7 ± 0.3	−4 ± 33	11703 ± 373	39.3 ± 1.3
3.0	3	624 ± 40	20.2 ± 0.1	7.1 ± 0.2	6.8 ± 0.2	−163 ± 35	11344 ± 328	38.6 ± 1.1
3.5	3	640 ± 43	12.8 ± 0.3	7.7 ± 0.2	7.7 ± 0.3	−300 ± 15	11062 ± 311	38.1 ± 1.0
4.0	3	638 ± 30		8.0 ± 0.1	8.5 ± 0.1	−623 ± 18	10514 ± 272	37.3 ± 0.9
4.5	3	623 ± 137		8.5 ± 0.6	9.2 ± 0.6	−753 ± 103	9869 ± 1155	35.6 ± 3.9
5.0	4	715 ± 272		9.6 ± 0.8	10.7 ± 0.7	−1051 ± 182	10248 ± 2634	37.9 ± 8.9
6.0	4	686 ± 170		10.0 ± 0.4	11.7 ± 0.4	−1420 ± 113	9175 ± 1607	35.5 ± 5.4

Results and Appendix) were used to estimate the unfolded ($[\theta]^{U}_{222}$) and folded ($[\theta]^{F}_{222}$) ellipticities as a function of temperature. Because residues 50−62 of the connector "hinge helix" are unfolded under all conditions investigated (*42*; see Appendix), their contribution to $[\theta]^{obs}_{222}$ is included in the folded state baseline $[\theta]^{F}_{222}$ as well as in the unfolded baseline $[\theta]^{U}_{222}$. (Any nonlinearity introduced into the folded state baseline by the presence of the hinge region is not detectible.)

A two-state model for the thermodynamics of unfolding was tested and found completely adequate to fit the unfolding data and obtain the observed equilibrium constant as a function of temperature or solute concentration.

$$K_{obs} = \left(\frac{[U]}{[F]}\right)_{eq} = \frac{f_U}{1 - f_U} \tag{11}$$

To examine the temperature dependence of various thermodynamic parameters under different solution conditions, nonlinear regression was performed using the SigmaPlot 2000 program to fit K_{obs} to the exponential form

$$K_{obs} = \exp\left(\frac{-\Delta H^{\circ}_{ref}}{RT} + \frac{\Delta S^{\circ}_{ref}}{R} + \frac{\Delta C^{\circ}_{P,obs}}{R}\left(\frac{T_{ref}}{T} - 1 + \ln\left(\frac{T}{T_{ref}}\right)\right)\right) \tag{12}$$

valid where $\Delta C^{\circ}_{P,obs}$ is independent of temperature. Inclusion of a linear dependence of $\Delta C^{\circ}_{P,obs}$on temperature does not improve the quality of the fits. In eq 12, T_{ref} is an arbitrary reference temperature (chosen to be 25 °C), and ΔH°_{ref} and ΔS°_{ref} are the fitted values of ΔH°_{obs} and ΔS°_{obs} at T_{ref}. Values of the characteristic temperatures T_S, T_H, T^{H}_{G}, and T^{C}_{G} were calculated from ΔH°_{ref}, ΔS°_{ref}, and $\Delta C^{\circ}_{P,obs}$. Alternatively, the data were fit to obtain $\Delta C^{\circ}_{P,obs}$, T_S, and T_H or to obtain $\Delta C^{\circ}_{P,obs}$, T_G, and $\Delta H^{\circ}_{obs}(T_G)$, the enthalpy of unfolding at T_G. In the latter parametrization, either T^{H}_{G} or T^{C}_{G} was selected for by constraining $\Delta H^{\circ}_{obs}(T_G)$ to be positive or negative, respectively. Values of the characteristic temperatures obtained directly from these fits were the same within uncertainty as those obtained indirectly from eq 12.

Calculation of ΔG°_{obs} of Unfolding in the Absence of Urea and the Urea Partition Coefficient K_P from Linear Extrapolation (LEM) and from the Local-Bulk Domain Model (LBDM). For the LEM analysis, values of ΔG°_{obs} as a function of C_3 at constant T were fit linearly to obtain $\Delta G^{\circ}_{obs}(m_3 = 0)$ and the *m*-value (eq 2). For the LBDM analysis, urea concentrations determined on the molar scale were converted to the molal concentration scale using the relation

$$m_3 \cong \frac{C_3 m_1^{\bullet} \bar{V}_1^{\bullet}}{1 - C_3 \bar{V}_3} \tag{13}$$

where $\bar{V}_1^{\bullet}$ and $\bar{V}_3$ are the molar volume of pure water and the partial molar volume of urea in water in units of L mol^{-1}, respectively. In applying eq 13, the dependence of $\bar{V}_3$ on C_3 was calculated by fitting a quartic polynomial to literature values of the apparent partial volume of urea ($\bar{V}_3^{app}$, evaluated assuming $\bar{V}_1$ is independent of urea concentration (*35*)) and calculating $\bar{V}_3$ from $\bar{V}_3^{app}$ by the standard method (*43*). In eq 13, neglect of the slight dependence of $\bar{V}_1$ on C_3 and of the small contributions of protein and K_2HPO_4 to the concentration scale conversion together contribute an error of less than 0.4% to the calculated values of m_3 (D.J.F., unpublished). If the concentration dependence of $\bar{V}_3$ were neglected, an additional error of ∼2% would be introduced.

In applying the LBDM to obtain $\Delta G^{\circ}_{obs}(m_3 = 0)$ and K_P, integral eq 6 also requires an expression for ϵ_3^m as a function of m_3 at each temperature of interest. Stokes (*35*) tabulated molal scale activity coefficients of urea in two-component aqueous solutions as a function of urea concentration at temperatures in the range 2−40 °C. For urea concentrations up to 12 m, values of ln γ_3^m at each temperature are best fit by a fourth degree polynomial in m_3:

$$\ln \gamma_3^m = \sum_{i=1}^{i=4} a_i m_3^i \tag{14}$$

Effects of temperature (2−40 °C) on ln γ_3 are well-fit by representing the coefficients a_1 and a_2 in eq 14 as a power series in temperature (K):

$$a_i = a_i^{(0)} + a_i^{(1)} T + a_i^{(2)} T^2 \qquad i = 1, 2 \tag{15}$$

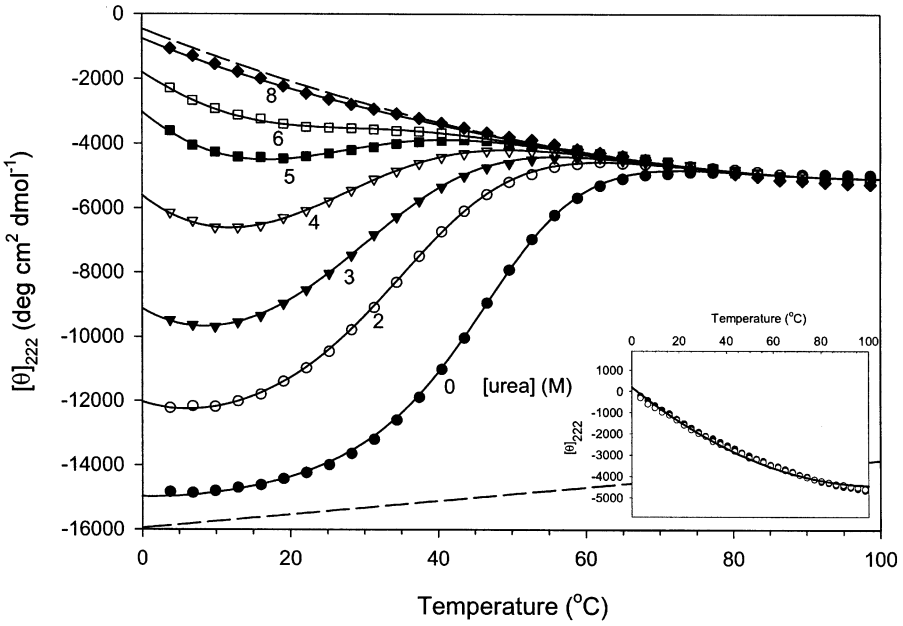

FIGURE 1: Thermal unfolding transitions of lacI HTH at representative urea concentrations (25 mM K_2HPO_4, pH 7.3). Averaged ellipticities $[\theta]_{222}$ (typically for 3−5 experiments; standard error ± 3%) are plotted vs temperature; regression fits were obtained using the two-state model with a constant $\Delta C^\circ_{P,obs}$ of unfolding (eqs 10−12; solid black lines) and the indicated baselines for the folded and unfolded states (dashed lines, cf. Appendix). The urea concentrations are 0 M (●), 2 M (○), 3 M (▼), 4 M (▽), 5 M (■), 6 M (□), and 8 M (◆). Inset compares the unfolded nonlinear baseline (−) with ellipticities determined for lacI HTH in 9.1 M urea (●) and proteinase K digests of lacI HTH in the absence of urea (○).

Values of these coefficients were obtained by fitting the data of Stokes (*35*): $a_1^{(0)} = -1.223 \pm 0.001$, $a_1^{(1)} = (6.801 \pm 0.006) \times 10^{-3}$, $a_1^{(2)} = (1.001 \pm 0.001) \times 10^{-5}$, $a_2^{(0)} = (7.271 \pm 0.012) \times 10^{-2}$, $a_2^{(1)} = -(3.949 \pm 0.008) \times 10^{-4}$, $a_2^{(2)} = (5.952 \pm 0.013) \times 10^{-7}$, $a_3 = (5.492 \pm 0.005) \times 10^{-4}$, $a_4 = (1.654 \pm 0.002) \times 10^{-5}$.

Differentiation of eq 14 with respect to ln m_3 to obtain ϵ_3^m and subsequent analytic integration of $(1 + \epsilon_3^m)(1 + K_P S_{1,3} m_3/m_1^\bullet)^{-1}$ (cf. eq 6) yields an analytic expression for ΔG°_{obs} as a function of m_3 which was fit to the data of Figures 1 and 4 (below) to obtain values of ΔG°_{obs} of unfolding in the absence of urea and of K_P for urea partitioning at each temperature examined. Values for b_1° and $S_{1,3}$ were fixed at 0.11 and 2.7 (cf. ref *31*) and $\Delta ASA = ASA^U = 3938$ Å^2, calculated as described below.

Calculation of Accessible Surface Area. The native state of the lacI DBD was taken from the first NMR model in the file 1LQC.PDB in the Protein Data Bank (www.rcsb.org). The denatured state was modeled as an extended β-chain using Insight II (Biosym Technologies) on an Octane workstation (Silicon Graphics). Both structures were truncated after 51 residues because the hinge region is found to be unstructured under all conditions examined (*42*). Water-accessible surface areas of these protein structures were calculated using a modification of the Richmond ANAREA program (*44*, *45*), with a probe radius of 1.4 Å and accepted values of the van der Waals radii (set I; *45*).

RESULTS

Dependence of Thermal Unfolding of the LacI HTH on Urea Concentration. To investigate the thermodynamic basis of stability of the lacI HTH and its dependence on urea concentration, thermal unfolding experiments were performed at urea concentrations from 0 to 9.1 M urea and monitored by circular dichroism spectroscopy at 222 nm. Averaged results of multiple experiments at representative urea concentrations in our standard 50 mM K^+ phosphate buffer (pH 7.3) are shown in Figure 1. The unfolding transition is observed to equilibrate rapidly on the experimental time scale allowing for thermal equilibration after each ∼3° temperature step. Data showed no signs of hysteresis, with transition curves obtained by scanning up in temperature overlaying those obtained by scanning down. The transition is independent of lacI DBD concentration over the 20-fold range examined (6−130 μM), and 95−100% reversible except at the highest temperatures examined, where reversibility was reduced to ∼90%.

Temperature-dependent baselines for the folded and unfolded states of the protein were established through a global regression procedure described in the appendix. The quadratic function describing the unfolded state as a function of temperature agrees closely with data for the lacI HTH collected at 9.1 M urea, demonstrating that the protein is unfolded at all temperatures at high urea concentrations. Thermal scans (in 50 mM K^+ without urea) of exhaustive proteinase K digests of the lacI HTH (predicted length ≤ 6 residues) overlay the thermal scans of lacI HTH in 9.1 M (Figure 1, inset), thereby providing further evidence for our conclusion that the unfolded state baseline is independent of urea concentration. To establish the temperature-dependent CD baseline for the folded state, not 100% populated at any temperature even in the absence of urea in our standard low-[salt] buffer (50 mM K^+; pH 7.3), data at high KCl concentrations were included in the global analysis (cf. Appendix). The resulting linear baseline is also shown in Figure 1.

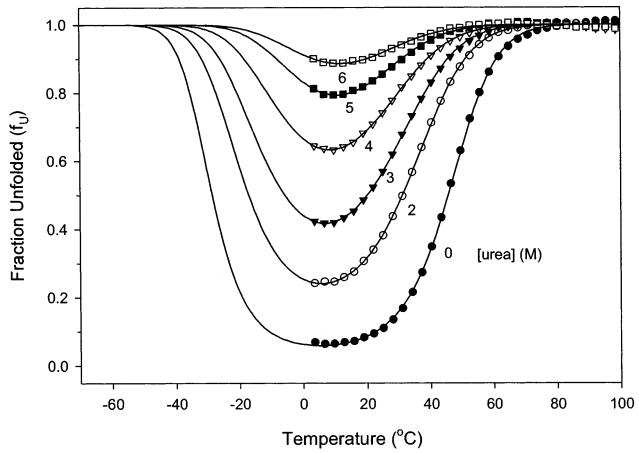

FIGURE 2: Fraction unfolded lacI HTH vs temperature. Data are from Figure 1, replotted as fraction unfolded (f_U) as a function of temperature. Regression fits to eqs 10−12 for two-state unfolding are shown. Symbols for different urea concentrations are the same as in Figure 1.

Our entire set of spectroscopic data for unfolding of this 49 residue HTH is completely consistent with a two-state thermodynamic model, as shown by the fitted curves in Figure 1. Individual HTH domains are either completely folded or completely unfolded at equilibrium, without detectible populations of intermediates. Each data set was fit separately to avoid imposing any restrictions on the functionality of the urea dependence of the thermodynamic parameters in the fits. Residues of the hinge region (50−62) exhibit no detectible structure under any conditions investigated here. In particular no unfolding transition for the hinge helix is observed, consistent with the conclusion (*42*) that this region folds upon binding to operator DNA. In addition to the downward shift in midpoint temperature of the thermal transition with increasing urea concentration, Figure 1 shows that the magnitude of $[\theta]_{222}^{obs}$ at the temperature of its relative minimum decreases with increasing C_3. Even in the absence of urea, the low-temperature data (<25 °C) exhibit a less negative $[\theta]_{222}^{obs}$ than that expected for the completely folded state of the HTH at these temperatures, deduced from studies at higher $[K^+]$ (see Appendix) and from estimates based on its amount of α-helix and other secondary structure (D.J.F., unpublished). We conclude that a small but significant fraction of the HTH population (∼6%) is unfolded even in the absence of urea at the temperature of maximum stability ($T_S = 7.8 \pm 1.5$ °C, where $\Delta S^\circ_{obs} = 0$). Therefore, unfolding studies at low $[K^+]$, interpreted by the two-state model using a folded state baseline determined at higher $[K^+]$, directly yield (without extrapolation) ΔG°_{obs} for unfolding over a wide temperature range (4−40 °C) in the absence of urea.

Results of the representative series of thermal denaturation experiments (Figure 1), normalized to fraction unfolded, are shown in Figure 2. The solid curves are fits to the two-state model of unfolding applied to the data using eqs 10−12; thermodynamic parameters from these fits are compiled in Table 1. The fits are extrapolated to lower (experimentally inaccessible) temperatures to emphasize the influence of cold-induced unfolding on the shape of the experimental curves. Although the midpoint temperatures of cold denaturation (T_G^C) are deduced to be substantially below the experimentally accessible temperature range (Figure 3), values of T_H (where $\Delta H^\circ_{obs} = 0$ and K_{obs} is a minimum) are well defined by the minima in $[\theta_{222}^{obs}]$ (Figure 1) and in the fraction unfolded (f_U) (Figure 2) in the range 6−10 °C. An increase in urea concentration destabilizes the folded state of the lacI HTH at all temperatures, causing both transition temperatures (T_G^H, T_G^C) to shift toward T_H, therefore reducing the difference $T_G^H - T_G^C$ that defines the window of thermal stability of the folded state.

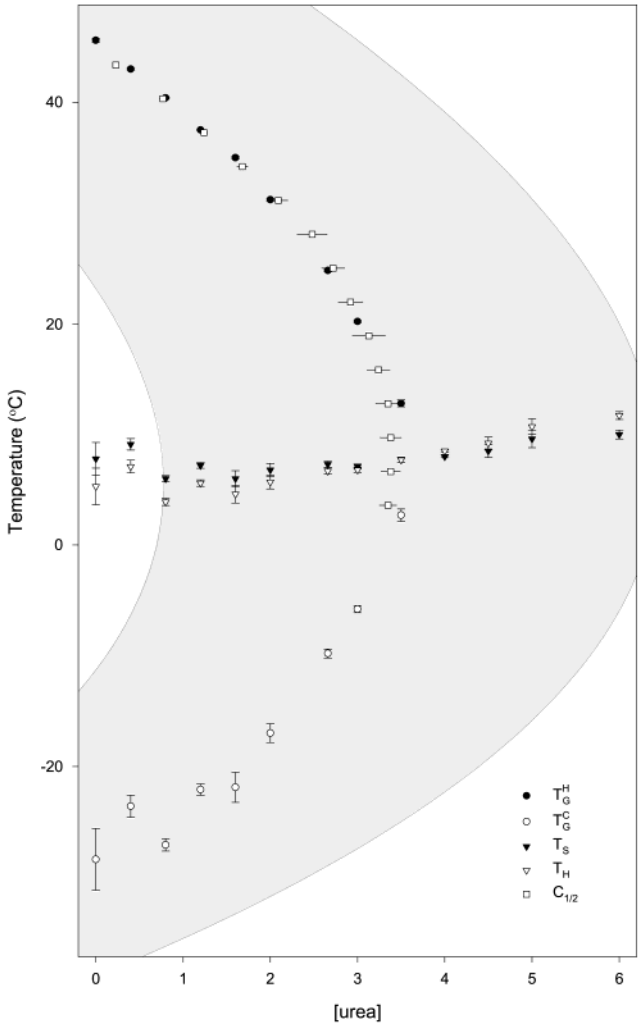

FIGURE 3: Temperature−urea phase diagram of lacI DBD unfolding. Values of T_G^H (●), T_G^C (○), and $C_{1/2}$ (□) define the phase boundary at which the folded and unfolded forms of the protein are equally populated. The shaded region depicts conditions where the extent of folding is between 10 and 90%. Also shown are the urea concentration dependences of T_S (▼), the temperature of maximal stability, and of T_H (▽), the temperature where K_{obs} is a minimum.

Figure 3 summarizes the dependence of fitted values of the high-temperature transition midpoint T_G^H on urea concentration. Also plotted in Figure 3 are predicted values of the lower transition midpoint temperature T_G^C obtained by extrapolation, assuming a temperature-independent $\Delta C^\circ_{P,obs}$. Together T_G^H and T_G^C determine the phase diagram of conditions where ΔG°_{obs} is zero (i.e., where the folded (F) and unfolded (U) states are equally populated). A mixed population of these two states exists at equilibrium over a wide range of urea concentrations and temperature; the

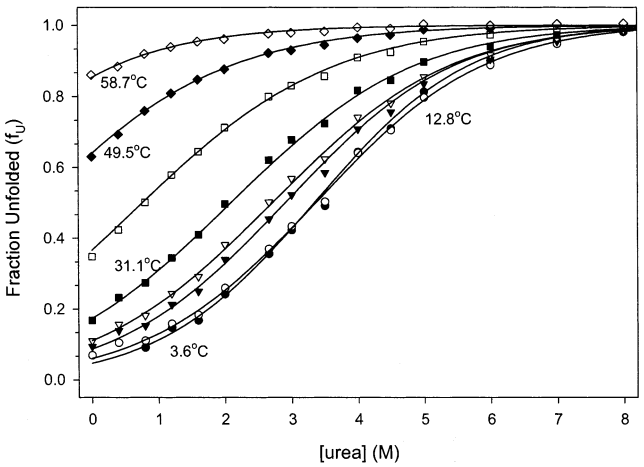

FIGURE 4: Isothermal urea-induced unfolding transitions of lacI DBD. Ellipticity data at temperatures of 3.6 °C (●), 12.8 °C (○), 22.0 °C (▼), 25.0 °C (▽), 31.1 °C (■), 40.3 °C (□), 49.5 °C (◆), and 58.7 °C (◇) as monitored by CD at 222 nm and converted to fraction unfolded (f_U) as described in the text. Fits to the local bulk domain model using eq 6 are shown as solid black lines.

shaded region in Figure 3 denotes the conditions in which both the folded and unfolded states are at least 10% populated (i.e., the region where ΔG°_{obs} is experimentally well-determined). With increasing urea concentration, the stability of the native state of the lacI HTH is reduced at all temperatures; T_G^H decreases and T_G^C is predicted to increase with increasing urea concentration. The two transition temperatures converge at ~3.5 M urea; above this urea concentration, the unfolded state is thermodynamically more stable than the folded state ($\Delta G^\circ_{obs} < 0$) at all temperatures.

Also plotted in Figure 3 are the characteristic temperatures T_H and T_S for this unfolding transition. At T_H, K_{obs} for unfolding is a minimum (cf. Table 1). At T_S, ΔG°_{obs} is a maximum. Both T_H and T_S increase with increasing urea concentration. The characteristic temperature T_H is predicted to increase linearly with increasing C_3 because ΔH°_{obs} of unfolding is found to decrease linearly with increasing C_3 (see Figure 5 below) and $\Delta C^\circ_{P,obs}$ of unfolding is independent of urea concentration:

$$\frac{dT_H}{dC_3} = -\frac{1}{\Delta C^\circ_{P,obs}}\left(\frac{\partial \Delta H^\circ_{obs}}{\partial C_3}\right)_T \quad (16)$$

The predicted value of this derivative (cf. Figure 5 below) is $dT_H/dC_3 = 1.05 \pm 0.14$ K M^{-1}, in complete agreement with the data of Figure 3.

The characteristic temperature T_S is predicted to increase nonlinearly with C_3:

$$\frac{dT_S}{dC_3} = -\frac{T_S}{\Delta C^\circ_{P,obs}}\left(\frac{\partial \Delta S^\circ_{obs}}{\partial C_3}\right)_T \quad (17)$$

Because $T\Delta S^\circ_{obs}$ is not as dependent on C_3 as is ΔH°_{obs}, T_S is predicted (from Figure 5 below) to be less dependent on C_3 than is T_H; over the measured range, eq 17 predicts that $dT_S/dC_3 = 0.30 \pm 0.15$ K M^{-1}, which is also consistent with the data of Figure 3. At urea concentrations less than 3.6 M, T_S exceeds T_H, as required for the folded state to be thermodynamically stable: $\Delta G^\circ_{obs}(T_S) = \Delta C^\circ_{P,obs}(T_S - T_H) > 0$. In the vicinity of 3.6 M urea, all four characteristic

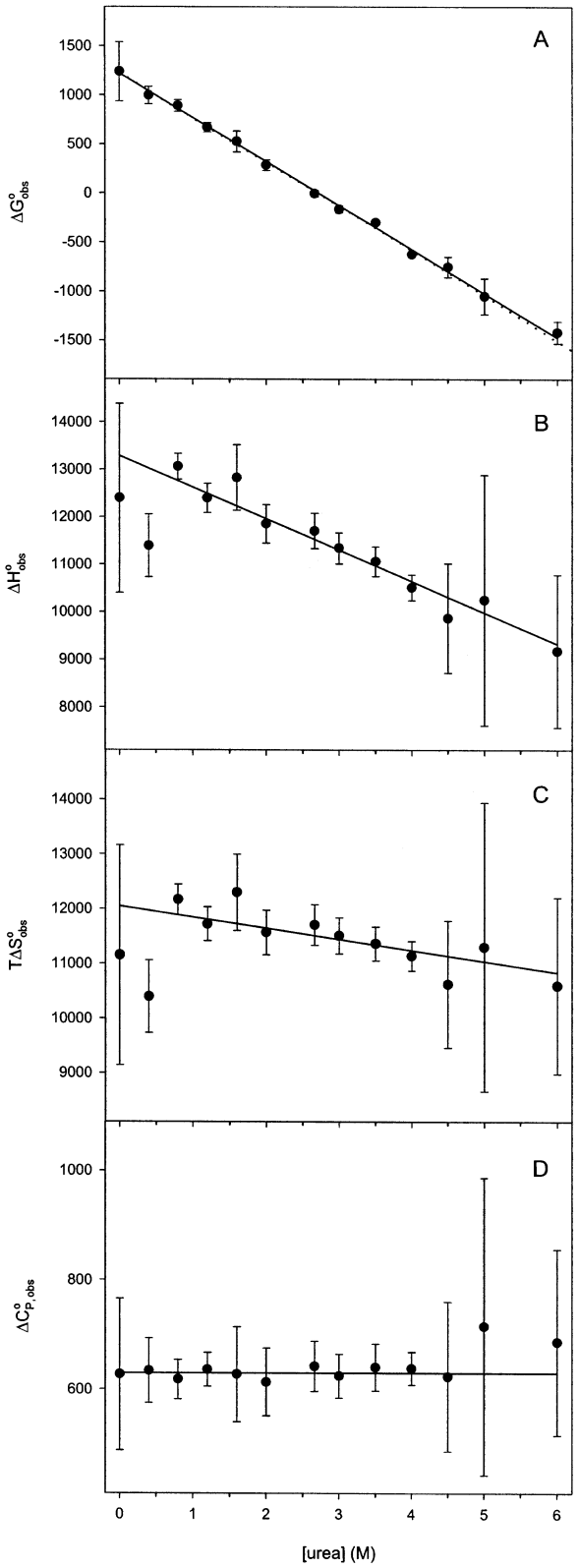

FIGURE 5: Thermodynamics of unfolding as a function of urea molarity. Panels A−D show the dependence of ΔG°_{obs}, ΔH°_{obs}, $T\Delta S^\circ_{obs}$, and $\Delta C^\circ_{P,obs}$ of denaturation on urea molarity at 25 °C. The dotted line in panel A represents a weighted fit to the LBDM using eqs 6 and 14−15. Solid lines represent weighted linear least-squares fits to the data in panels A−C with slopes $(\partial \Delta G^\circ_{obs}/\partial C_3)_{T=25°C} = -449 \pm 11$ cal mol^{-1} M^{-1}, $(\partial \Delta H^\circ_{obs}/\partial C_3)_{T=25°C} = -661 \pm 90$ cal mol^{-1} M^{-1}, and $(\partial T\Delta S^\circ_{obs}/\partial C_3)_{T=25°C} = -203 \pm 91$ cal mol^{-1} M^{-1} for the dependence of ΔG°_{obs}, ΔH°_{obs}, and ΔS°_{obs} on urea, respectively. The solid line in D gives the weighted mean value of $\Delta C^\circ_{P,obs}$ (630 ± 50 cal mol^{-1} K^{-1}).

Table 2: Temperature Dependence of the Parameters from LEM and LBDM Analysis

	LEM		LBDM analysis		direct
T (°C)	$\Delta G^\circ_{obs}(C_3 = 0)$ (cal mol^{-1})	m-value (cal mol^{-1} M^{-1})	$\Delta G^\circ_{obs}(C_3 = 0)$ (cal mol^{-1})	K_P	$\Delta G^\circ_{obs}(C_3 = 0)$ (cal mol^{-1})
3.6	1616 ± 39	481.8 ± 8.2	1655 ± 42	1.126 ± 0.002	1435 ± 415
6.7	1587 ± 40	470.0 ± 8.7	1627 ± 44	1.120 ± 0.002	1494 ± 442
9.7	1567 ± 44	463.3 ± 9.6	1593 ± 46	1.116 ± 0.002	1502 ± 409
12.8	1536 ± 51	458.3 ± 10.6	1559 ± 53	1.112 ± 0.003	1481 ± 408
15.8	1515 ± 50	467.6 ± 10.5	1535 ± 51	1.113 ± 0.003	1470 ± 401
18.9	1476 ± 81	471.2 ± 10.8	1492 ± 83	1.111 ± 0.003	1398 ± 374
22.0	1359 ± 58	466.1 ± 10.3	1376 ± 60	1.109 ± 0.002	1331 ± 349
25.0	1222 ± 52	449.0 ± 10.8	1233 ± 52	1.103 ± 0.003	1240 ± 301
28.1	1135 ± 74	456.9 ± 8.8	1146 ± 75	1.103 ± 0.002	1114 ± 253
31.1	937 ± 47	448.4 ± 9.2	943 ± 47	1.099 ± 0.002	968 ± 222
34.2	736 ± 20	437.8 ± 9.2	745 ± 20	1.096 ± 0.002	791 ± 189
37.3	551 ± 16	442.5 ± 9.4	557 ± 16	1.095 ± 0.002	603 ± 150
40.3	337 ± 13	440.4 ± 10.5	342 ± 13	1.094 ± 0.002	392 ± 134

temperatures become equal ($T_H = T_S = T_G^H = T_G^S \cong 7.7$ °C). Above 3.6 M urea, T_H exceeds T_S, and the folded state is thermodynamically unstable at all temperatures.

Isothermal Urea-Concentration Dependence of Stability of the LacI HTH and its Enthalpic and Entropic Components. Because thermal transition data were taken at the same set of temperatures (~3 °C intervals), they can equally well be represented as isothermal urea titrations at these temperatures. Figure 4 summarizes that part of our urea−temperature data set not shown in Figure 1. Like the thermal transitions of Figure 2, these urea-induced unfolding transitions are very broad. For typical globular proteins, urea-induced unfolding at pH 7 is observable only at urea concentrations above 4 M. For the lacI HTH, however, urea-induced unfolding spans the range of urea concentrations from 0 to ~7 M. Midpoint urea concentrations, $C_{1/2}$, of the isothermal urea-induced unfolding transitions obtained from isothermal fits to the LBDM (eq 6), are plotted in Figure 3. As expected, values of $C_{1/2}$ as a function of temperature, obtained from isothermal LBDM fits, describe the same stability curve in Figure 3 as values of T_G^H obtained from fits of thermal transition data to the constant−$\Delta C^\circ_{P,obs}$ van't Hoff equation (eq 12) at each urea concentration investigated. Thus, the overlap of the urea unfolding transitions at 3.6 and 12.8 °C (Figure 4) is explained simply by the proximity of these temperatures to T_S.

The urea dependence of ΔG°_{obs} at 25 °C is plotted in Figure 5A. The extreme breadth of the urea-induced unfolding transition (Figure 4) allows ΔG°_{obs} to be determined directly at this temperature from 0 to 6 M urea; ΔG°_{obs} varies linearly with urea concentration over this range with a slope (the negative of the m-value) of −449 ± 11 cal mol^{-1} M^{-1} (solid line fit in Figure 5A); ΔG°_{obs} is also a linear function of urea molarity at all other temperatures where this dependence can be quantified (4−40 °C; cf. Table 2).

The enthalpic and entropic contributions to ΔG°_{obs} as a function of urea molarity and temperature were determined from analysis of K_{obs} using eq 12 (with $T_{ref} = 25$ °C). At 25 °C, in the absence of urea, both ΔH°_{obs} (12.4 ± 2.0 kcal mol^{-1}) and $T\Delta S^\circ_{obs}$ are positive and large relative to ΔG°_{obs}. Figure 5B,C shows that both ΔH°_{obs} and $T\Delta S^\circ_{obs}$ decrease linearly with increasing urea molarity at 25 °C, with derivatives $(\partial\Delta H^\circ_{obs}/\partial C_3)_{T,P} = -661 \pm 90$ cal mol^{-1} M^{-1} and $(\partial T\Delta S^\circ_{obs}/\partial C_3)_{T,P} = -203 \pm 91$ cal mol^{-1} M^{-1}. Because ΔH°_{obs} decreases more rapidly with increasing urea concentration than $T\Delta S^\circ_{obs}$, ΔH°_{obs} and $T\Delta S^\circ_{obs}$ intersect at the midpoint urea concentration for unfolding at 25 °C ($C_{1/2}$ of 2.72 ± 0.13 M). Heat capacity changes $\Delta C^\circ_{P,obs}$ are also obtained from the regression fit to eq 12. Figure 5D indicates that $\Delta C^\circ_{P,obs}$ is independent of urea concentration within error, with an average value of 630 ± 50 cal mol^{-1} K^{-1}.

Temperature Dependences of the m-Value and of $(\partial \ln K_{obs}/\partial C_3)_T$ for Unfolding the lacI HTH; Implications for Linkages between Temperature and Urea Derivatives of Thermodynamic Functions of Unfolding. The systematic temperature dependence of the lacI HTH m-value in the range of our experiments (4−40 °C) is shown in Figure 6A. Within the uncertainty, the m-value decreases linearly with increasing temperature:

$$\left(\frac{\partial m\text{-value}}{\partial T}\right)_{C_3} = -\frac{\partial}{\partial T}\left(\frac{\partial \Delta G^\circ_{obs}}{\partial C_3}\right)_T = 1.02 \pm 0.22 \text{ cal mol}^{-1}\text{ M}^{-1}\text{ K}^{-1}$$

The closely related quantity $(\partial \ln K_{obs}/\partial C_3)_T = m\text{-value}/RT$ is plotted vs temperature in Figure 6B. Within the uncertainty, $(\partial \ln K_{obs}/\partial C_3)_T$ also decreases linearly with increasing temperature:

$$\frac{\partial}{\partial T}\left(\frac{\partial \ln K_{obs}}{\partial C_3}\right)_T = -(4.41 \pm 0.4) \times 10^{-3}\text{ M}^{-1}\text{ K}^{-1}$$

Nonlinearity in Figure 6A and/or B arising from the fact that the two derivatives $(\partial m\text{-value}/\partial T)_{C_3}$ and $\partial(\partial \ln K_{obs}/\partial C_3)/\partial T$ cannot both be independent of temperature is not detectible given the experimental uncertainty, as discussed below.

Obligate thermodynamic linkages (eqs 7 and 8) relate the temperature dependences of the m-value and of $(\partial \ln K_{obs}/\partial C_3)_T$ to the urea concentration dependences of ΔS°_{obs} and ΔH°_{obs}, respectively. At 25 °C, from Figure 5C $(\partial\Delta S^\circ_{obs}/\partial C_3)_T = -0.68 \pm 0.31$ cal mol^{-1} K^{-1} M^{-1}. From Figure 6A, $(\partial m\text{-value}/\partial T)_{C_3} = -1.02 \pm 0.22$ cal mol^{-1} K^{-1} M^{-1}. Although the uncertainty is rather large, these two derivatives are equal within error, as required by eq 8. Likewise, from Figure 5B, at 25 °C, $(1/RT^2)(\partial\Delta H^\circ_{obs}/\partial C_3)_T = -(3.74 \pm 0.51) \times 10^{-3}$ M^{-1} K^{-1} and from Figure 6B, $\partial(\partial \ln K_{obs}/\partial C_3)/\partial T = -(4.41 \pm 0.4) \times 10^{-3}$ M^{-1} K^{-1}. Within the uncertainty, these two quantities are equal, as required by eq 7.

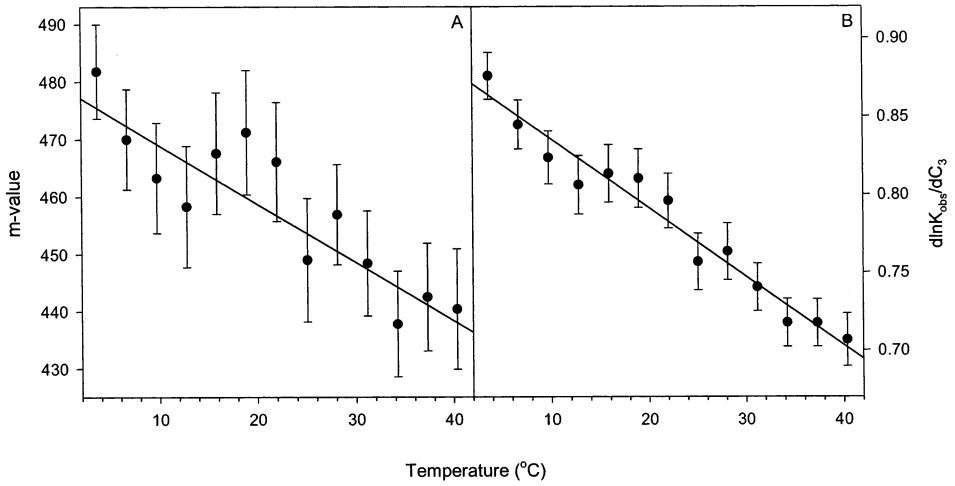

FIGURE 6: The dependence of the *m*-value (panel A) and $(\partial \ln K_{obs}/\partial C_3)_T$ (panel B) on temperature. The weighted linear least-squares fits in panels A and B have slopes $(\partial m\text{-value}/\partial T)_{C_3} = -1.02 \pm 0.22$ cal mol^{-1} K^{-1} M^{-1} and $\partial/\partial T(\partial \ln K_{obs}/\partial C_3)_T = -(4.41 \pm 0.4) \times 10^{-3}$ M^{-1} K^{-1}.

Figure 5D indicates that $\Delta C^\circ_{P,obs}$ is independent of C_3 within the experimental uncertainty. Interpreted by the linkage relation (eq 9), if $\Delta C^\circ_{P,obs}$ is independent of C_3 then both $(\partial \Delta H^\circ_{obs}/\partial C_3)_T$ and $(\partial \Delta S^\circ_{obs}/\partial C_3)_T$ are independent of temperature. In this situation, the *m*-value must be a linear function of temperature (Figure 6A) and the temperature dependence of $(\partial \ln K_{obs}/\partial C_3)_T$ (Figure 6B) is predicted to be nonlinear. However, experimental uncertainty makes it impossible to detect small deviations from linearity over the 40 °C temperature range examined in Figure 6A,B. Values of $(\partial \Delta C^\circ_{P,obs}/\partial C_3)_T$ in the range from −11 to +21 cal mol^{-1} K^{-1} M^{-1} result in insignificant curvature of both panels of Figure 6; curvature introduced by a stronger urea concentration dependence of $\Delta C^\circ_{P,obs}$ should be apparent outside the scatter in the data. This conclusion is consistent with the observation (Figure 5D) that $\Delta C^\circ_{P,obs}$ is independent of urea concentration (0−6 M) within uncertainty ($\Delta C^\circ_{P,obs} = 630 \pm 50$ cal mol^{-1} K^{-1}) implying that $|(\partial \Delta C^\circ_{P,obs}/\partial C_3)_T|$ does not exceed 21 cal mol^{-1} K^{-1} M^{-1}. We interpret this negligibly small dependence of $\Delta C^\circ_{P,obs}$ on C_3 to indicate that the ΔASA of unfolding in urea is independent of urea concentration and that the accumulation of urea in the vicinity of protein surface does not significantly affect the interaction of nonpolar surface with water, which is the dominant contributor to $\Delta C^\circ_{P,obs}$.

DISCUSSION

The lacI DBD as a Model Protein For Investigating Effects of Solutes on Unfolding Thermodynamics. At neutral pH and in the absence of denaturants, both the maximum thermodynamic stability ($\Delta G^\circ_{obs} = 1.59 \pm 0.05$ kcal at $T_S = 7.8 \pm 1.0$ °C) and the thermal stability ($T^H_G = 45.6$ °C) of lacI HTH are significantly less than those of other globular proteins. In addition, both the thermal unfolding transition and the isothermal urea unfolding transitions are very broad: $(df_U/dT)^{-1} = 32$ °C at T^H_G in the absence of urea and $(df_U/dC_3)^{-1} = 5.3$ M at $C_{1/2}$ and 25 °C. Both T_H and T_S are in the experimentally accessible range at all urea concentrations investigated. These characteristics are very desirable for the investigation of solute effects on the thermodynamics of protein unfolding by van't Hoff methods because K_{obs} can be determined over wide ranges of temperature and urea concentration including the temperature T_H where K_{obs} is a maximum. In such situations, analysis of the temperature dependence of K_{obs} by eqs 11−12 yields accurate values of ΔH°_{obs}, ΔS°_{obs}, and $\Delta C^\circ_{P,obs}$ as functions of urea concentration and of the temperature dependence of the *m*-value. These desirable characteristics result in large part from the small size of the folding domain (49 residues in the HTH) and the consequently small amount of buried ASA (3938 Å^2). Thermodynamic investigations have been carried out on a number of other small proteins which lack disulfide cross-links and stabilizing ligands, including proteins with largely beta structure such as Btk (*46*) and α-spectrin SH3 domains (*47*), proteins with both alpha and beta structure (e.g., B1 and B2 domains from protein G (*48*) and chymotrypsin inhibitor 2 (*49*)), and entirely alpha helical homeodomain (*50*−*52*) and phage repressor proteins (*53*, *54*). With the probable exception of the homeodomain DNA-binding proteins discussed below, all of these proteins, although only slightly larger than lacI HTH, are significantly more stable (both thermodynamically and thermally) than lacI HTH at neutral pH (cf. Table 3). It is interesting to compare the stability of lacI HTH to that of DNA-binding domains of homeodomain and phage repressor proteins that also contain HTH motifs. While repressor proteins with a five-helix fold (phage 434 cro protein, monomeric lambda repressor) are significantly more stable than lacI HTH, homeodomain proteins such as vnd/NK-1 and MATα2, which like lacI HTH contain only three helices, have similar thermal stability to lacI HTH (and most likely similar thermodynamic stability, although the thermodynamics of unfolding have not been fully characterized for these latter proteins). The lower thermodynamic stability of the three-helix HTH domains, which stems in part from the lower packing efficiency (and reduced burial of surface area per residue) of these HTH proteins relative to the five-helix phage proteins, may play an important functional role by reducing the thermodynamic cost of conformational adaptation at the protein-operator interface in recognizing different operator sequences (*8*−*10*, *13*).

Table 3: Thermal and Thermodynamic Stability for a Representative Group of Small Globular Proteins

protein	N_{res}	T_G^H (°C)	$\Delta H^\circ_{obs}(T_G^H)$ (kcal mol^{-1})	$\Delta C^\circ_{P,obs}$ (cal K^{-1} mol^{-1})	T_S (°C)	$\Delta G^\circ_{obs}(T_S)$ (kcal mol^{-1})	pH	buffer and salt conc	ref
lacI HTH	49	45.6	25.3	0.63	7.8	1.6	7.3	50 mM KP_i	this study
	49	80.0	42.2	0.63	19.0	3.8		50 mM KP_i, 2.0 M KCl	
protein G B1	56	87.5	61.7	0.62	0.7	7.8	5.4	50 mM NaAc	(*48*)
protein G B2	56	79.4	56.9	0.69	6.2	6.1	5.4	50 mM NaAc	
chymotrypsin inhibitor 2	64	73.8	67.0	0.72	−7.8	8.2	3.5	50 mM MES	(*49*)
Btk-SH3	67	74.0	48.0	0.78	17.6	4.0	7.0	30 mM NaP_i	(*46*)
α-spectrin SH3	57	65.8	47.1	0.67	2.3	4.6	4.0	10 mM NaAc	(*47*)
monomeric λ repressor	80	57.2	68.0	1.44	13.2	4.6	8.0	20 mM KP_i, 100 mM NaCl	(*53*)
434 cro protein	71	57.0	46.6	0.98	12.8	3.2	6.0	25 mM KP_i, 100 mM KCl	(*72*)
MATα2 HD	72	56.3	32.5				7.0	20 mM NaP_i	(*51*)
		61.4	41.6					20 mM NaP_i, 300 mM NaCl	
vnd/NK-2 HD	80	35.8	19.0				7.4	50 mM HEPES	(*50*)
		52.0	42.0					50 mM HEPES, 500 mM NaCl	
TTF-1 HD	61	42.8	25.4				7.0	10 mM Pi, 100 mM NaF	(*52*)

An additional factor contributing to the low stability of the lacI HTH is the moderately low salt concentration (50 mM K^+; phosphate buffer) of our studies. As shown in the appendix, the stability of lacI HTH increases strongly with increasing KCl concentration; at 2 M KCl, $T_G^H = 80$ °C and regression analysis of the thermal unfolding curve for a two-state model, assuming that $\Delta C^\circ_{P,obs}$ is independent of KCl concentration and temperature, yields an estimate of ΔG°_{obs} of ∼3.8 kcal mol^{-1} at 25 °C, comparable to other small, un-cross-linked proteins (cf. Table 3). Hence, charge repulsions in the folded state or interactions in the unfolded state (internal ion pairing or salt bridging) at 50 mM K^+ destabilize the folded state of the lacI HTH by ∼2.6 kcal mol^{-1} relative to 2 M KCl. A strong salt-dependence of thermal stability has also been observed in the structurally similar vnd/NK-2 (*50*) and MATα2 (*51*) homeodomains.

The small free energy difference between the folded and unfolded ensembles of the lacI HTH, even at or below 25 °C, means that a measurable fraction of the population remains in the unfolded state under these conditions and hence allows direct measurement of the thermodynamics of unfolding. Moreover, both $\Delta\Gamma_{\mu_3}$ and ΔH°_{obs} are relatively small, resulting in very broad transitions as a function of urea concentration and of temperature. In the absence of urea, ΔG°_{obs} for denaturation is experimentally measurable over more than a 60 °C temperature range including both characteristic temperatures T_H and T_S, a feature which is essential for accurate van't Hoff determination of the $\Delta C^\circ_{P,obs}$ for the process. These properties of the system allow us to examine the urea concentration dependence of ΔG°_{obs}, ΔH°_{obs}, $T\Delta S^\circ_{obs}$, and $\Delta C^\circ_{P,obs}$ over wider ranges of temperature and urea concentrations than are accessible with other proteins. Hence, the lacI DBD is an ideal model system for studying the effects of denaturants and other small solutes that affect protein stability.

For larger, more stable proteins, destabilizing conditions such as acidic pH (*47*, *54*) or high denaturant concentrations (*24*, *53*, *55*, *56*) are required to allow direct experimental determination of K_{obs} at T_H. Larger proteins with larger ΔASAs of unfolding typically exhibit stronger dependences of ΔG°_{obs} on denaturant concentrations (i.e., larger *m*-values, because the *m*-value is proportional to ΔASA (*17*, *31*)) that limit such experiments to a much narrower range of denaturant concentrations than are accessible with the lacI HTH. However, in situations in which T_G^C is shifted into the experimentally accessible temperature range using urea or another denaturant, the range of temperatures where K_{obs} is directly measurable can be very large, even if the range of denaturant concentrations accessible at fixed temperature is not. For example, at a urea concentration of 4 M, K_{obs} for HPr unfolding is measurable without extrapolation over a 50 °C range in temperature (*24*), a much wider temperature range than is normally accessible in typical protein unfolding experiments and comparable to the temperature range over which K_{obs} is directly measurable for lacI HTH at all urea concentrations.

The Dependence of ΔG°_{obs} on Urea Molarity: Direct Tests of the LEM and LBDM. The marginal stability of the lacI HTH allows the first direct determination of ΔG°_{obs} and the *m*-value for unfolding of a globular protein at urea concentrations between 0 and 6 M at neutral pH and over a wide temperature range including 25 °C. Previously, only for the unfolding of alanine-based α-helical peptides were ΔG°_{obs} and the *m*-value determined directly at low urea concentrations at 25 °C and neutral pH. In that study, Scholtz, Baldwin, and co-workers (*34*) concluded that the free energy of helix propagation increased linearly with urea molarity between 0 and 3.6 M urea. Investigations of the denaturant (urea or GuHCl) concentration dependence of ΔG°_{obs} for protein unfolding at low denaturant concentration were performed on more stable proteins than lacI HTH and therefore required use of either high temperature or low pH to destabilize the native protein. In general, these studies observed a linear dependence of ΔG°_{obs} on denaturant concentration under the conditions investigated. However, extrapolations of these results to 25 °C and neutral pH have been controversial, typically requiring assumptions regarding the effects of temperature or pH on the *m*-value and/or the effect of denaturant concentration on the $\Delta C^\circ_{P,obs}$ of unfolding. For some proteins, these extrapolations predict linearity of ΔG°_{obs} vs denaturant concentration at 25 °C and neutral pH (e.g., *23*, *24*); for others, significant curvature and a denaturant-concentration-dependent *m*-value are predicted (e.g., *25*, *26*, *57*).

For globular proteins, the present study of the lacI HTH provides the first direct test of the LEM at physiological temperatures and neutral pH. In accord with the result obtained with α-helical peptides from 0 to 3.6 M urea, we find that ΔG°_{obs} for unfolding the lacI HTH is a linear function of the molar scale urea concentration from 0 to 6

M urea. Both these studies argue for the validity of the LEM to determine intrinsic values of the stability of protein and peptides. Consistent with our previous conclusion for other globular proteins (*31*), the *m*-value/ΔASA ratio for lacI HTH (0.11) is approximately 25% as large as that calculated for the Scholtz-Baldwin peptides. The 4-fold larger *m*-value/ΔASA ratio for α-helix disruption as compared to protein unfolding correlates with the calculated 4-fold larger contribution of polar peptide backbone to the ΔASA of unfolding an alanine-based α-helix (52 vs 14% for lacI HTH) and suggests that unfolding in both systems is driven primarily by accumulation of urea in the vicinity of polar peptide backbone surface.

The linear dependence of ΔG°_{obs} on urea concentration in the molar range (Figure 5A), with no evidence of curvature or saturation at the highest urea concentration examined, is indicative of a favorable weak preferential interaction between urea and the exposed protein surface (*31*). Site binding models (in which ΔN_{urea} independent sites for urea with binding constant K_{urea} are exposed upon unfolding) can account for this observed linearity; the dependence of ΔG°_{obs} on urea predicted by these models, $\Delta\Delta G^\circ_{obs} = -\Delta N_{urea} RT \ln(1 + K_{urea} a_{urea})$, can be approximated by the linear term in a Taylor series expansion in the limit of very weak binding, i.e., ΔG°_{obs} is a linear function of urea activity ($\Delta\Delta G^\circ_{obs} = -\Delta N_{urea} RTK_{urea} a_{urea}$). Solvent exchange binding models show a similar limiting behavior (*34*, *58*). Such an interpretation is not very informative as one cannot independently determine the site binding constant and number of sites but only their product. Furthermore, since a plot of ΔG°_{obs} vs urea concentration shows no evidence of saturation even at high solute concentrations, no justification exists for treating the interaction of urea with protein surface as a stoichiometric binding process. Therefore, we interpret our results in the context of the LBDM (*31*, *37*, *38*), which treats the interaction of urea with protein surface as a local accumulation of urea relative to its bulk concentration. Previous work from this laboratory (*31*) found that the LBDM yielded a near-linear dependence of ΔG°_{obs} on C_3 over the range of urea concentrations examined here if the local-bulk urea partition coefficient (K_P) and stoichiometry of urea−H_2O exchange at the protein surface ($S_{1,3}$) are independent of urea concentration. Indeed, the local-bulk thermodynamic analysis provides a quantitative fit to the urea-induced unfolding data (dotted line in Figure 5A), thereby providing direct experimental justification for the use of the LEM and the assumption of a urea-concentration-independent *m*-value.

For the surface exposed on unfolding the lacI HTH, the urea local-bulk partition coefficient, K_P, is found to be 1.103 ± 0.002 at 25 °C, in close agreement with the value obtained by a global analysis of protein folding data, 1.12 ± 0.01 (*31*), and with the value for native protein surface, 1.10 ± 0.04 (*39*). Thus, according to this model, the average concentration of urea in the local domain surrounding that surface of the protein exposed on unfolding is only slightly greater than its concentration in bulk solution (a ratio of 1.1), yet this slight accumulation completely explains the phenomenon of urea-induced unfolding.

Temperature Dependence of the m-Value: Interpretation Using Linkage Relations and the Local-Bulk Domain Model. We find that the *m*-value and the related quantity $\partial \ln K_{obs}/\partial C_3$ for unfolding of the lacI HTH with urea both *decrease* with increasing temperature (cf. Figure 6). The data of Nicholson and Scholtz (*24*) for unfolding of HPr protein are consistent with this behavior. This small but significant temperature-dependence of the *m*-value is most fundamentally interpreted using linkage relationships (eqs 7−8), which are general and model-independent thermodynamic results. From eqs 7−8, it can be seen that the *m*-value must depend on temperature whenever ΔS°_{obs} depends on urea concentration, while the derivative $\partial \ln K_{obs}/\partial C_3$ must depend on temperature whenever ΔH°_{obs} depends on urea concentration. Hence, the reductions in *m*-value and in $\partial \ln K_{obs}/\partial C_3$ with increasing temperature for the unfolding of lacI HTH and HPr most fundamentally reflect the unfavorable entropy change and favorable enthalpy change, respectively, associated with accumulation of urea in the vicinity of that protein surface exposed upon unfolding. Previous thermodynamic studies of the interactions of urea with protein surface also concluded that these weak interactions are enthalpically driven and opposed by an unfavorable entropy of interaction (*24*, *59*, *60*).

The LBDM interpretation of the *m*-value (eq 5) indicates three possible origins of its observed temperature dependence: the partition coefficient K_P, the amount of water in the local domain ($B_1^\circ = b_1^\circ \, ASA^{U'}$) and/or the urea activity coefficient derivative ϵ_3^m. From the data of Stokes (*35*), analyzed by eqs 14−15, we conclude that ϵ_3^m increases significantly with increasing temperature; the increase in $(1 + \epsilon_3^m)$ over the temperature range 4−40 °C is half as large in magnitude as the observed decrease in *m*-value over this temperature. This temperature dependence is incorporated in the LBDM analysis described below. In the absence of any information regarding the temperature dependence of the amount of local water (B_1°), which could result from temperature dependences of $ASA^{U'}$ and/or b_1°, we propose that the temperature dependence of the *m*-value (corrected for that of ϵ_3^m) indicates a temperature dependence of the local-bulk partition coefficient of urea (K_P).

Values of K_P in the range 3.6 to 40.3 °C were obtained from fits of eq 6 to experimental data for ΔG°_{obs} as a function of ϵ_3^m (see Methods). Fitted values of K_P are compiled in Table 2 and plotted vs temperature in Figure 7. A van't Hoff plot of ln K_{obs} vs reciprocal Kelvin temperature (Figure 7 inset) is linear, indicating that the enthalpy of partitioning is independent of temperature. From nonlinear fitting of the temperature dependence of K_P (Figure 7), assuming that the enthalpy and entropy of partitioning are independent of temperature, we find that accumulation of urea in the vicinity of the lacI DBD surface exposed upon unfolding, to the extent that the average surface concentration exceeds the bulk by 10.3% at 25 °C, is enthalpically driven ($\Delta H_P^\circ = -131 \pm 6$ cal mol^{-1}) with a smaller unfavorable entropic term ($\Delta S_P^\circ = -0.24 \pm 0.02$ eu). Interpretation of the reported dependence of ΔH°_{obs} and ΔS°_{obs} on urea concentration for HPr (*24*) in the context of the local bulk domain model yields values of ΔH°_{obs} and ΔS°_{obs} that are within the uncertainty of our results for lacI HTH.

The effects of urea on the solubilities of model compounds that mimic various protein functional groups have been

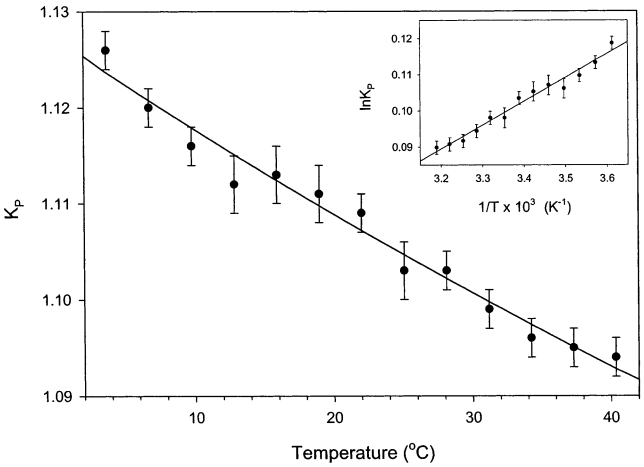

FIGURE 7: Temperature dependence of the local bulk partition coefficient of urea (K_P). The continuous line represents a van't Hoff fit to the data assuming ΔH_P does not depend on temperature. Inset: Van't Hoff plot of ln K_P vs $1/T$ (K).

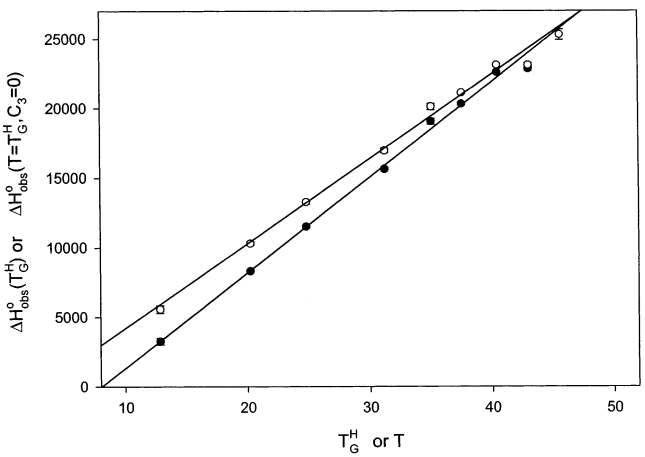

FIGURE 8: The dependence of ΔH°_{obs} on temperature. Solid circles are values of $\Delta H^\circ_{obs}(T^H_G)$ plotted as a function of T^H_G. Open circles are calculated values of ΔH°_{obs} at the same temperature but in the absence of urea obtained from $\Delta H^\circ_{obs}(T^H_G)$ using eq 19.

extensively reported in the literature (*61*−*66*). Recently, phase equilibrium perturbation calorimetry has been used to directly measure the effects of urea on enthalpies of dissolution in saturated solutions of various diketopiperazines (*67*). Although these data can be interpreted in terms of preferential interactions and the local-bulk model, a quantitative comparison must take into account the different constraints on the system (constant chemical potential of the model compound, rather than constant concentration) and potential effects from self-interactions of the model compound at the higher concentrations used in these studies. We are currently investigating the assumptions involved in such a comparison in the context of the local bulk domain model (Felitsky et al., in progress).

The alternative interpretation of the temperature dependence of the *m*-value in terms of a temperature-dependent hydration or ASA cannot be ruled out. An increase in local structural fluctuations with increasing temperature would increase the average surface exposure of both the folded and unfolded ensembles. However, only if such a thermal expansion were more significant in the folded state, leading to an overall net decrease in $\Delta\text{ASA} = \text{ASA}^{U'}$ of unfolding, could this effect contribute significantly to the observed behavior of the *m*-value as a function of temperature. Effects of pH on urea *m*-values have previously been interpreted in terms of an increase in ΔASA with decreasing pH (*68*, *69*) but may also involve effects similar to those discussed above, including any pH dependence of the ϵ_3^m and of the urea partition coefficient K_P and/or a urea-concentration dependence of protein pK_a values.

Obtaining the Intrinsic $\Delta C^\circ_{P,obs}$ of Unfolding from Analysis of $\Delta H^\circ_{obs}(T^H_G)$ as a Function of T^H_G, Varied Using Urea Concentration. Because of the difficulty in determining $\Delta C^\circ_{P,obs}$ of protein unfolding directly from the difference in pre- and post-transition baselines in differential scanning calorimetry experiments, $\Delta C^\circ_{P,obs}$ has often been estimated from the slope of a plot of $\Delta H^\circ_{obs}(T^H_G)$ vs T^H_G, where the T^H_G is shifted by altering the concentration of a denaturant such as pH or urea. However, if ΔH°_{obs} varies with the concentration of the chemical perturbant, estimates of $\Delta C^\circ_{P,obs}$ using this method will be systematically in error. In calorimetric studies using pH to perturb T^H_G, the enthalpic contribution to ΔH°_{obs} from protonation has been internally compensated using buffer matching of protonation enthalpies (*70*). No analogous compensation is possible for enthalpic effects of urea and other cosolvent denaturants, so they have been little used in this regard. In what follows, we use our lacI HTH thermodynamic data to conclude that even for a cosolvent such as urea where the perturbing effect is largely enthalpic, the dependence of the transition enthalpy, $\Delta H^\circ_{obs}(T^H_G)$, on the transition temperature T^H_G (perturbed using urea concentration) provides a reasonable estimate of the intrinsic $\Delta C^\circ_{P,obs}$ of unfolding.

At any specified temperature, values of ΔH°_{obs} in the absence of urea can be obtained from $\Delta H^\circ_{obs}(T^H_G)$ by integrating over C_3:

$$\Delta H^\circ_{obs}(T = T^H_G, C_3 = 0) = \Delta H^\circ_{obs}(T^H_G, C_3) - \int_0^{C_3} \left(\frac{\partial \Delta H^\circ_{obs}}{\partial C_3}\right)_{T=T_GH} \partial C_3$$

$$= \Delta H^\circ_{obs}(T^H_G, C_3) - C_3\left(\frac{\partial \Delta H^\circ_{obs}}{\partial C_3}\right)_{T=25°C} \quad (19)$$

For lacI HTH, evaluation of the integral is straightforward because the derivative $(\partial \Delta H^\circ_{obs}/\partial C_3)_T$ is independent of both C_3 (see Figure 5) and temperature. The latter conclusion follows from the linkage relation of eq 9 and the finding (Figure 5) that $\Delta C^\circ_{P,obs}$ is independent of C_3, within the experimental uncertainty.

Figure 8 plots values of the van't Hoff unfolding transition enthalpy $\Delta H^\circ_{obs}(T^H_G)$ (closed circles) and values of ΔH°_{obs} at the same series of temperatures corrected to zero urea concentration (i.e., $\Delta H^\circ_{obs}(T = T^H_G, C_3 = 0)$) (open circles) as a function of transition temperature T^H_G perturbed using urea concentration. Both plots are linear with experimental uncertainty, and intersect at the T^H_G in the absence of urea. The linearity of the plot of $\Delta H^\circ_{obs}(T = T^H_G, C_3 = 0)$ vs temperature provides additional evidence that $\Delta C^\circ_{P,obs}$ is independent of temperature in the range examined. The

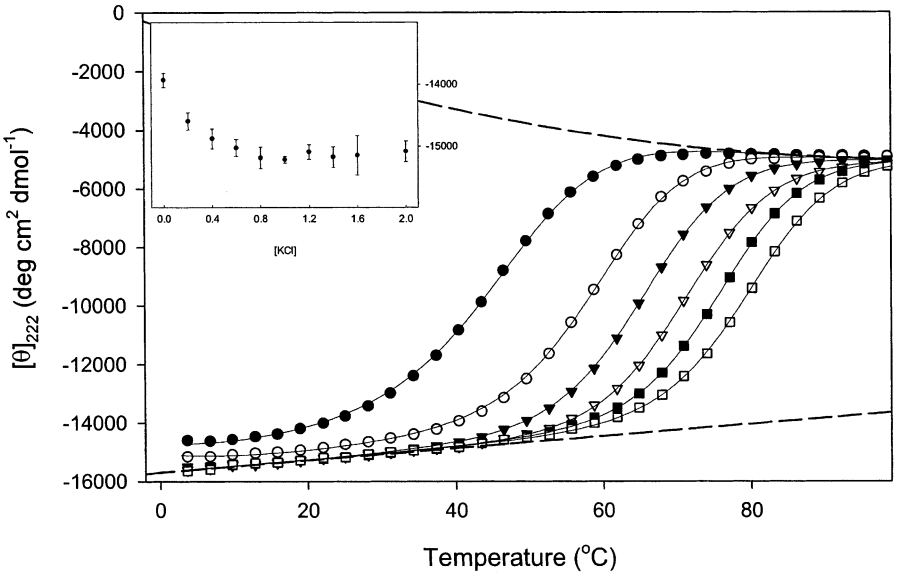

FIGURE 9: Thermal unfolding transitions of lacI HTH at different KCl concentrations (25 mM K_2HPO_4, pH 7.3). Averaged ellipticities $[\theta]_{222}$ are plotted vs temperature. The KCl concentrations are 0 M (●), 0.4 M (○), 0.8 M (▼), 1.2 M (▽), 1.6 M (■) and 2 M (□). Inset: plot of $[\theta]_{222}$ vs KCl concentration at 25 °C.

slopes of these plots only differ by 12%, indicating that the quantity $d\Delta H^\circ_{obs}(T^H_G)/dT^H_G$, obtained using urea as the perturbant, yields an estimate of $\Delta C^\circ_{P,obs}$ accurate to within 10−15%, comparable to that with which $\Delta C^\circ_{P,obs}$ is usually determined.

The general thermodynamic relationship between the experimentally determined derivative $d\Delta H^\circ_{obs}(T^H_G)/dT^H_G$, and the $\Delta C^\circ_{P,obs}$ of denaturation is:

$$\frac{d\Delta H^\circ_{obs}(T^H_G)}{dT^H_G} = \Delta C^\circ_{P,obs} + \frac{(\partial \Delta H^\circ_{obs}/\partial C_3)_T}{dT^H_G/dC_3} \qquad (20)$$

Equation 20 quantifies the expectation that a hypothetical denaturant which affects primarily the ΔS°_{obs} of unfolding, so that $|(\partial \Delta H^\circ_{obs}/\partial C_3)_T| \ll |dT^H_G/dC_3|$, would be optimal to use to estimate $\Delta C^\circ_{P,obs}$ from $d\Delta H^\circ_{obs}(T^H_G)/dT^H_G$. For lacI HTH, even though ΔH°_{obs} of unfolding decreases significantly with increasing urea concentration ($(\partial \Delta H^\circ_{obs}/\partial C_3)_T = -661 \pm 90$ cal mol^{-1} M^{-1}), the contribution of this term to the difference between $\Delta H^\circ_{obs}(T^H_G)$ and $\Delta H^\circ_{obs}(T = T^H_G, C_3 = 0)$ (eq 19) and to the difference between $d\Delta H^\circ_{obs}(T^H_G)/dT^H_G$ and $\Delta C^\circ_{P,obs}$ (eq 20) is relatively small. Studies of guanidinium chloride unfolding (*55*) and sarcosine stabilization (*71*) of proteins also report dependences of ΔH°_{obs} on C_3 for these solutes that, through eq 19 and 20, would give small corrections to $d\Delta H^\circ_{obs}(T^H_G)/dT^H_G$ as an estimate of the intrinsic $\Delta C^\circ_{P,obs}$. We conclude that $\Delta C^\circ_{P,obs}$ can generally be estimated from plots of $\Delta H^\circ_{obs}(T^H_G)$ vs T^H_G to within the 10−15% error to which it is normally determined. However, curvature in such plots may not indicate a temperature dependent $\Delta C^\circ_{P,obs}$ since dT^H_G/dC_3 (cf. eq 20) is a function of urea concentration and $(\partial \Delta H^\circ_{obs}/\partial C_3)_T$ may, in general, depend on temperature for other solutes or systems.

CONCLUSIONS

The marginal thermodynamic and thermal stability of the lacI HTH have allowed us to characterize the urea concentration dependence of ΔG°_{obs}, ΔH°_{obs}, $T\Delta S^\circ_{obs}$, and $\Delta C^\circ_{P,obs}$ over wider ranges of temperature and urea concentrations than are accessible for most protein systems. We find that our entire data set is consistent with the widely used linear extrapolation model (LEM) and can be well interpreted using the local-bulk domain model (LBDM). We also demonstrate the fundamental role of linkage relationships in interpreting many of the measurable thermodynamic quantities discussed herein including the observed negative temperature dependence of the *m*-value, which reflects the unfavorable dependence of ΔS°_{obs} on urea concentration. This type of extended data set on the thermodynamics of unfolding for a small globular protein should prove valuable in testing and analysis of semiempirical and theoretical models based on urea effects on solubility, calorimetry, and other model system data; it further provides an experimental data set on a small protein which should be more tractable in computational studies of these interactions. The same properties that make lacI HTH valuable in analyzing urea induced denaturation make it a favorable model system for studying the effects of other solutes on protein unfolding. Studies of this type are in progress to characterize the interaction of Hofmeister ions, osmolytes, and crowding agents with protein surface, which will provide insight into the enthalpic and entropic components of these interactions.

ACKNOWLEDGMENT

The authors thank Dr. Darrell McCaslin for technical assistance with the CD spectrometer, Drs. Robert Kaptein and Christian Spronk for supplying the recombinant lacI DBD cell strain used in these experiments, Dr. Nick Pace, Dr. R. L. Baldwin, and the anonymous reviewers for their comments, Dr. Elizabeth Courtenay for helpful discussions, and Sheila Aiello for help in preparation of the manuscript. D.J.F. was supported in part as a NSF predoctoral fellow and as a NIH Molecular Biosciences trainee.

APPENDIX

The interpretation of spectroscopic measurements of denaturation necessitates the selection of baselines represent-

ing the folded and unfolded states of the protein. Since thermal transitions of proteins and peptides are broad, these baselines generally have to be extrapolated over a large portion of the experimental temperature range. To accurately establish these baselines, we have used KCl and urea concentrations as variables to shift the thermal transition of the lacI HTH over a 90 °C range of temperatures. The universal CD baseline for the unfolded state of lacI HTH is well established from thermal scans at high urea concentrations (cf. Figure 1, inset). In this appendix, the CD signal for the folded state of the lacI DBD is established by examining thermal scans over a range of KCl concentrations.

Figure 9 shows a series of thermal unfolding data over the range of KCl concentrations investigated. Above ~80 °C, data at all KCl concentrations examined approach the same post-transition baseline as that observed in the urea studies in Figure 1. Addition of KCl strongly stabilizes the native state of the protein, shifting T_G^H to higher temperatures with increasing KCl concentration. Above ~0.8 M KCl, values of $[\theta]_{222}$ in the pretransition region increase linearly with increasing temperature but are independent of KCl (and urea; data not shown) concentration and therefore allow us to establish a universal native state baseline for this protein. From 0.05 to 0.8 M K^+, the apparent baseline decreases with increasing salt concentration (Figure 9, inset), indicating that deviations from this universal baseline at lower KCl concentrations (and in the presence of urea; cf Figure 1) result from an observable equilibrium population of unfolded protein molecules.

The pretransition and post-transition baselines established by the data in Figures 1 and 9 are well-modeled by empirical linear and quadratic curves, respectively:

$$\frac{[\theta]_{222}^{F,T}}{[\theta]_{222}^{F,25°C}} = 1 + \alpha_0(T - 25\ °C)$$
$$\frac{[\theta]_{222}^{U,T}}{[\theta]_{222}^{U,25°C}} = 1 + \alpha_1(T - 25\ °C) + \alpha_2(T - 25\ °C)^2 \quad \text{(A1)}$$

The parameters α_i were determined by globally fitting data at all urea and KCl concentrations examined, with a separate set of eqs A1 for each set of solution conditions but a single set of values for the parameters α_i. A linear temperature dependence of the pretransition baseline for lacI HTH, with little or no dependence on urea concentration, is consistent with observations on a wide variety of other proteins (*24*, *46*, *47*, *55*). Almost without exception, a linear temperature dependence of the post-transition baseline has also been assumed in previous studies. In the present study, the post-transition baseline is obtained over a much wider temperature range, demonstrating the need for a quadratic fit.

REFERENCES

1. Lewis, M., Chang, G., Horton, N. C., Kercher, M. A., Pace, H. C., Schumacher, M. A., Brennan, R. G., and Lu, P. Z. (1996) *Science 271*, 1247−1254.
2. Levandoski, M. M., Tsodikov, O. V., Frank, D. E., Melcher, S. E., Saecker, R. M., and Record, M. T. (1996) *J. Mol. Biol. 260*, 697−717.
3. Tsodikov, O. V., Saecker, R. M., Melcher, S. E., Levandoski, M. M., Frank, D. E., Capp, M. W., and Record, M. T. (1999) *J. Mol. Biol. 294*, 639−655.
4. Law, S. M., Bellomy, G. R., Schlax, P. J., and Record, M. T. (1993) *J. Mol. Biol. 230*, 161−173.
5. Muller, J., Oehler, S., and MullerHill, B. (1996) *J. Mol. Biol. 257*, 21−29.
6. Spolar, R. S., and Record, M. T. (1994) *Science 263*, 777−784.
7. Spronk, C. A. E. M., Slijper, M., vanBoom, J. H., Kaptein, R., and Boelens, R. (1996) *Nat. Struct. Biol. 3*, 916−919.
8. Mossing, M. C., and Record, M. T. (1985) *J. Mol. Biol. 186*, 295−305.
9. Kalodimos, C. G., Bonvin, A. M. J. J., Salinas, R. K., Wechselberger, R., Boelens, R., and Kaptein, R. (2002) *EMBO J. 21*, 2866−2876.
10. Frank, D. E., Saecker, R. M., Bond, J. P., Capp, M. W., Tsodikov, O. V., Melcher, S. E., Levandoski, M. M., and Record, M. T. (1997) *J. Mol. Biol. 267*, 1186−1206.
11. Spronk, C. A., Bonvin, A. M., Radha, P. K., Melacini, G., Boelens, R., and Kaptein, R. (1999) *Struct. Fold Des. 7*, 1483−1492.
12. Kalodimos, C. G., Folkers, G. E., Boelens, R., and Kaptein, R. (2001) *Proc. Natl. Acad. Sci. U.S.A. 98*, 6039−6044.
13. Spronk, C. A., Folkers, G. E., Noordman, A. M., Wechselberger, R., van den Brink, N., Boelens, R., and Kaptein, R. (1999) *EMBO J. 18*, 6472−6480.
14. Kalodimos, C. G., Boelens, R., and Kaptein, R. (2002) *Nat. Struct. Biol. 9*, 193−197.
15. Kalodimos, C. G., Folkers, G. E., Boelens, R., and Kaptein, R. (2001) *Proc. Natl. Acad. Sci. U.S.A. 98*, 6039−6044.
16. Pace, C. N., and Shaw, K. L. (2000) *Proteins*, 1−7.
17. Myers, J. K., Pace, C. N., and Scholtz, J. M. (1995) *Protein Sci. 4*, 2138−2148.
18. Dalby, P. A., Oliveberg, M., and Fersht, A. R. (1998) *J. Mol. Biol. 276*, 625−646.
19. Wrabl, J., and Shortle, D. (1999) *Nat. Struct. Biol. 6*, 876−883.
20. Shortle, D., and Meeker, A. K. (1986) *Proteins 1*, 81−89.
21. Pace, C. N., Laurents, D. V., and Erickson, R. E. (1992) *Biochemistry 31*, 2728−2734.
22. Greene, R. F., and Pace, C. N. (1974) *J. Biol. Chem. 249*, 5388−5393.
23. Santoro, M. M., and Bolen, D. W. (1992) *Biochemistry 31*, 4901−4907.
24. Nicholson, E. M., and Scholtz, J. M. (1996) *Biochemistry 35*, 11369−11378.
25. Johnson, C. M., and Fersht, A. R. (1995) *Biochemistry 34*, 6795−6804.
26. Wu, J. W., and Wang, Z. X. (1999) *Protein Sci. 8*, 2090−2097.
27. Wyman, J. (1964) *Adv. Protein Chem. 19*, 223−286.
28. Schellman, J. A. (1994) *Biopolymers 34*, 1015−1026.
29. Timasheff, S. N. (1998) *Adv. Protein Chem. 51*, 355−432.
30. Record, M. T., Zhang, W. T., and Anderson, C. F. (1998) *Adv. Protein Chem. 51*, 281−353.
31. Courtenay, E. S., Capp, M. W., Saecker, R. M., and Record, M. T. (2000) *Proteins 41*, 72−85.
32. Aune, K. C., and Tanford, C. (1969) *Biochemistry 8*, 4586−4590.
33. Schellman, J. A. (1990) *Biophys. Chem. 37*, 121−140.
34. Scholtz, J. M., Barrick, D., York, E. J., Stewart, J. M., and Baldwin, R. L. (1995) *Proc. Natl. Acad. Sci. U.S.A. 92*, 185−189.
35. Stokes, R. H. (1967) *Aust. J. Chem. 20*, 2087−2100.
36. Pace, C. N. (1975) *CRC Crit. Rev. Biochem. 3*, 1−43.
37. Record, M. T., and Anderson, C. F. (1995) *Biophys. J. 68*, 786−794.
38. Courtenay, E. S., Capp, M. W., Anderson, C. F., and Record, M. T. (2000) *Biochemistry 39*, 4455−4471.
39. Courtenay, E. S., Capp, M. W., and Record, M. T. (2001) *Protein Sci. 10*, 2485−2497.
40. Slijper, M., Boelens, R., Davis, A. L., Konings, R. N., van der Marel, G. A., van Boom, J. H., and Kaptein, R. (1997) *Biochemistry 36*, 249−54.
41. Woody, R. W. (1995) *Methods Enzymol. 246*, 34−71.
42. Spronk, C. A., Slijper, M., van Boom, J. H., Kaptein, R., and Boelens, R. (1996) *Nat. Struct. Biol. 3*, 916−9.
43. Klotz, I. M., and Rosenberg, R. M. (1994) *Chemical Thermodynamics*, 5th ed., John Wiley & Sons, Inc., New York.
44. Richmond, T. J. (1984) *J. Mol. Biol. 178*, 63−89.
45. Livingstone, J. R., Spolar, R. S., and Record, M. T. (1991) *Biochemistry 30*, 4237−4244.
46. Knapp, S., Mattson, P. T., Christova, P., Berndt, K. D., Karshikoff, A., Vihinen, M., Smith, C. I. E., and Ladenstein, R. (1998) *Proteins 31*, 309−319.
47. Viguera, A. R., Martinez, J. C., Filimonov, V. V., Mateo, P. L., and Serrano, L. (1994) *Biochemistry 33*, 2142−2150.

48. Alexander, P., Fahnestock, S., Lee, T., Orban, J., and Bryan, P. (1992) *Biochemistry 31*, 3597−3603.
49. Jackson, S. E., and Fersht, A. R. (1991) *Biochemistry 30*, 10428−10435.
50. Gonzalez, M., Weiler, S., Ferretti, J. A., and Ginsburg, A. (2001) *Biochemistry 40*, 4923−4931.
51. Carra, J. H., and Privalov, P. L. (1997) *Biochemistry 36*, 526−535.
52. Damante, G., Tell, G., Leonardi, A., Fogolari, F., Bortolotti, N., Dilauro, R., and Formisano, S. (1994) *FEBS Lett. 354*, 293−296.
53. Huang, G. W. S., and Oas, T. G. (1996) *Biochemistry 35*, 6173−6180.
54. Padmanabhan, S., Laurents, D. V., Fernandez, A. M., Elias-Arnanz, M., Ruiz-Sanz, J., Mateo, P. L., Rico, M., and Filimonov, V. V. (1999) *Biochemistry 38*, 15536−15547.
55. Agashe, V. R., and Udgaonkar, J. B. (1995) *Biochemistry 34*, 3286−3299.
56. Ibarra-Molero, B., Makhatadze, G. I., and Sanchez-Ruiz, J. M. (1999) *Biochim. Biophys. Acta 1429*, 384−390.
57. Pace, C. N., and Vanderburg, K. E. (1979) *Biochemistry 18*, 288−292.
58. Schellman, J. A., and Gassner, N. C. (1996) *Biophys. Chem. 59*, 259−275.
59. Makhatadze, G. I., and Privalov, P. L. (1992) *J. Mol. Biol. 226*, 491−505.
60. Zolkiewski, M., Nosworthy, N. J., and Ginsburg, A. (1995) *Protein Sci. 4*, 1544−1552.
61. Sijpkes, A. H., Vandekleut, G. J., and Gill, S. C. (1993) *Biophys. Chem. 46*, 171−177.
62. Sijpkes, A. H., Vandekleut, G. J., and Gill, S. C. (1994) *Biophys. Chem. 52*, 75−82.
63. Nozaki, Y., and Tanford, C. (1963) *J. Biol. Chem. 238*, 4074−4081.
64. Nandi, P. K., and Robinson, D. R. (1984) *Biochemistry 23*, 6661−6668.
65. Schonert, H., and Stroth, L. (1981) *Biopolymers 20*, 817−831.
66. Robinson, D. R., and Jencks, W. P. (1965) *J. Am. Chem. Soc. 87*, 2462−2470.
67. Zou, Q., Habermann-Rottinghaus, S. M., and Murphy, K. P. (1998) *Proteins Struct. Funct. Genet. 31*, 107−115.
68. Pace, C. N., Laurents, D. V., and Thomson, J. A. (1990) *Biochemistry 29*, 2564−2572.
69. Pace, C. N., Laurents, D. V., and Erickson, R. E. (1992) *Biochemistry 31*, 2728−2734.
70. Privalov, P. L. (1979) *Adv. Protein Chem. 33*, 167−241.
71. Del Pino, I. M. P., and Sanchez-Ruiz, J. M. (1995) *Biochemistry 34*, 8621−8630.
72. Padmanabhan, S., Laurents, D. V., Fernandez, A. M., Elias-Arnanz, M., Ruiz-Sanz, J., Mateo, P. L., Rico, M., and Filimonov, V. V. (1999) *Biochemistry 38*, 15536−47.

BI0270992